JUACEP Program 2021-2022 at UCLA & PolyMTL

Japan-US-Canada Collaborative Education Program

Nagoya University

Table of Contents

\<1\> About the Program

1-1. Overview

Nagoya University's JUACEP provides two course options for students at the Graduate School of Engineering to study abroad: the medium-term (up to six months) course and the long-term (more than eight months) course. Choosing one of those courses, the selected students are offered an opportunity to work together with faculty and other researchers or students from all over the world at the world's top universities.

Each student works on a research project related to his own master's thesis topic while belonging to a specialized research group of the partner universities in the United States and Canada. As of 2022, Partners are University of Michigan (UM), UCLA, University of Toronto (UT), North Carolina State University (NCSU) and Polytechnique Montréal (PolyMTL).

In addition to research implementation, the students are expected to attend the group seminars, the group discussions and other events. At the end of each course, the students are required to submit research reports to their mentors at the host institution, and after returning to Nagoya, give research presentations based on their achievements in front of the faculty and peer students at JUACEP Workshop held in Nagoya University. The report and the presentation are primary requisites to be accredited for the program completion.

This publication is compiling the activities of the following students.
[a] One student of long-term course from October 2021 to June 2022 at UCLA.
[b] One student of medium-term course from May 2022 to September 2022 at Polytechnique Montréal.
[c] Two students of medium-term course from August 2022 to February 2023 at UCLA.

JUACEP outbound 2021-2022 Medium- and Long-term Courses Flowchart

	[a] Long-term 2021 at UCLA	[b] Medium-term 2022 at POLYMTL	[c] Medium-term 2022 at UCLA
March 2021	Approach to UCLA faculty and accepted		
	Prepare for *VGR and J1 visa		
October	Leave Japan for the US and start the program		
January 2022		Apply to POLY	
February		Accept the screening result	
March		Prepare for the staying qualification	Approach to UCLA faculty and accepted
May		Leave Japan for Canada and start the program	Prepare for *VGR and J1 visa
June	Return to Japan		
August	Achievement presentation *27th Workshop, Aug. 23, 2022*		Leave Japan for the US and start the program
September		Return to Japan	
October		Achievement presentation *28th Workshop, Oct. 6, 2022*	
February 2023			Return to Japan
March			Achievement presentation *29th Workshop, Mar. 14, 2023*

*VGR: Visiting Graduate Researcher for UCLA

1-2. Participants

[a] 2021 Long-term course at UCLA
Program period: October 25, 2021 - June 25, 2022

Yusuke Terai 寺井　勇裕	M1	Prof. Noritsugu Umehara Micro-Nano Mechanical Science and Engineering	Prof. Ya-Hong Xie Materials Science and Engineering, UCLA

[b] 2022 Medium-term course at Polytechnique Montréal
Program period: May 13, 2022 - September 6, 2022

Hirofumi Amada 天田　裕文	M1	Prof. Yutaka Matsuo Chemical Systems Engineering	Prof. Fabio Cicoira Chemical Engineering, POLY

[c] 2022 Medium-term course at UCLA
Program period：August 30, 2022 - February 1, 2023

Kentaro TAKAGI 高木 健太郎	M1	Assoc.Prof. Toru ASAI Mechanical Systems Engineering	Prof.Tetsuya Iwasaki Mechanical & Aerospace Engineering, UCLA

Program period：September 19, 2022 - February 23, 2023

Hiroshi Goto 後藤　拓	M1	Assist.Prof. Hisaaki TANAKA Applied Physics	Prof. Kang L. Wang Electrical & Computer Engineering, UCLA

Coordinator

UCLA	Prof. Jenn-Ming Yang Materials Science and Engineering
PolyMTL	Ms. Julie Defretin Stratigic Advisor, POINT

JUACEP Members

Prof. Yang Ju	Micro-Nano Mechanical Science and Engineering
Prof. Noritsugu Umehara	Micro-Nano Mechanical Science and Engineering
Prof. Toshiro Matsumoto	Mechanical Systems Engineering
Prof. Yasumasa Ito	G30 Automotive Engineering
Assoc. Prof. Takayuki Tokoroyama	Micro-Nano Mechanical Science and Engineering
Assoc. Prof. Dina Grib	International Academic Exchange Office
Tomoko Kato, Administrative staff	JUACEP Office

JUACEP Office
Room #341, Engineering Building 2, Nagoya University
Furo-cho, Chikusa-ku, Nagoya 4648603　　Phone +81 (0)52 789 2799
https://www.juacep.engg.nagoya-u.ac.jp

⟨2⟩ Research Reports and Presentations

2-1.   **2021 Long-term course at UCLA**

October 25, 2021 - June 25, 2022

[Research Report]
Yusuke Terai, *mentored by Prof. Ya-Hong Xie, Materials Science and Engineering, UCLA*,
"Bio-sample droplet evaporation with LASER irradiation to induce salt precipitation aside and improve SERS throughput"   …P.8

[Presentation at the 27th JUACEP Workshop, August 26, 2022]
          …P.15

Bio-sample droplet evaporation with LASER irradiation to induce salt precipitation aside and improve SERS throughput

Yusuke Terai

Department of Micro-Nano Mechanical Science and Engineering, Graduate school of Engineering, Nagoya University
terai@ume.mech.nagoya-u.ac.jp

Supervisor: Prof. Ya-Hong Xie

Department of Materials science and Engineering, University of California-Los Angeles
yhx@ucla.edu

Abstract

In this work, the method to improve throughput of SERS spectrum of biomarker is studied. The biological sample consists of biomarker such as exosome and buffered solution. We drop the biological sample solution on SERS substrate and let it evaporate, then get the SERS spectrum of target biomarkers. However, salt precipitation derived from buffered solution disturb SERS spectrum of the target biomarker. To avoid this problem, we established LASER evaporation method which induces salt crystallization on LASER radiation point while biomarker isn't affected. This method is surprisingly applied to only Au pyramid substrate not to Au or Si flat substrate. We concluded this is because plasmonic effect and the method can be widely available on biological samples for SERS.

1. Introduction

Exosomes are the most abundant and best-characterized type of EVs, ranging from 30 to 200 nm in diameter. They are produced via the endosomal pathway and are released into the extracellular space from multivesicular bodies [1] Exosomes have role in spreading of diseases throughout the affected tissue [2]-[6] and are a valuable source of biomarkers for diagnosing various diseases, containing cancer and neurodegenerative diseases.

Raman spectroscopy is a widely used, label-free, non-destructive method. It has been used for extracting spectroscopic information originating from chemical bonding in molecules, which can in turn be used as fingerprints by which molecules are identified[7]. In addition, with metallic particles or nanostructured metallic surfaces, Raman signals become much higher due to plasmonic effect, which is known as surface-enhanced Raman spectroscopy (SERS)[8]-[11]. This makes them extremely useful for studying biomolecules and single molecules, which otherwise go undetected under conventional Raman spectroscopy. Some researchers used Raman spectroscopy especially SERS with Au pyramid[12].

The goal of this project will be to contribute to disease diagnosis via advancing biosensing based on SERS Identification of Molecules (SIM). In quantitative terms, this project will focus on increasing the number of usable SERS spectra of the samples (particularly exosomes). To that end, a surface plasmonic assisted technique of controlling the precipitation process is studied. A key challenge in achieving that is the salt precipitation derived from buffered solution, wherein the salt dendrites and crystals cover up a major portion of the Au-nanopyramid substrate. This in term limits the area available for plasmonic interaction and signal enhancement of the biomarkers. Therefore, we need easy method to improve throughput of SERS spectrum of biomarkers that can help control the precipitation process, and in turn improve plasmon-assisted SERS signal enhancement, which would ultimately yield higher number of usable SERS spectra with high Signal-Noise Ratio.

The samples studied are suspensions, and a key concept in the drying process of suspensions is the "Coffee-Ring Effect", which basically refers to the ring-like deposits on surfaces after suspensions, such as coffees, dry up. After suspension droplet evaporate, the deposition is non-uniform. When a spilled droplet of suspension dries on a solid surface, it leaves a dense, ring-like deposit along the perimeter. Such ring deposits are common wherever drops containing dispersed solids evaporate on a surface, and they influence processes such as printing, washing and coating. This phenomenon is called coffee ring[13]. The insight of coffee ring can apply to our study. Coffee ring can form under two main physics phenomena. One is pinning effect that causes contact line pinning. Pinning effect is what keeps the droplet contact line. If the solid surface is ideally flat, smooth, and chemically homogeneous, the contact angle is determined by Young's equation in equation (1),

$$\gamma_{LV}\cos\theta = \gamma_{SV} - \gamma_{SL} \qquad (1)$$

However, It's nothing but an ideal and it's generally known that contact angle has hysteresis[14]-[16] in the practical surface, especially, surface roughness and chemical heterogeneity. Contact angle hysteresis is expressed as advancing angle minus receding angle. Advancing angle is

the maximum contact angle droplet can be while holding the contact line. Receding contact angle is the minimum contact angle droplet can be while holding the contact line. Therefore, pinning effect and contact angle hysteresis have a strong relationship. The strong pinning effect keeps the contact line even if the droplet volume changes, thus increasing the range of contact angles that can be taken. The insight is also related to coffee ring because the droplet evaporation means contact angle becoming lower. The other physical phenomenon to explain coffee ring is evaporation flux on the droplet surface. Evaporation flux is the highest near the edge of the droplet. This fact is proved by equations and computational simulation as shown in Figure 1 [13],[17]-[21][26].
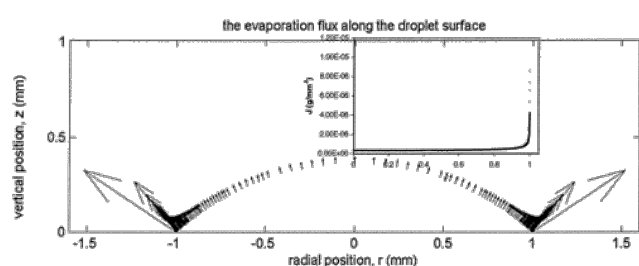
Figure 1 Evaporation flux along the droplet surface. [17]

Due to these two physics phenomena, the out-forward flow arises from the canter to compensate the lost water volume and maintain droplet spherical shape. Therefore, suspended particles move toward the edge on the outward flow, then precipitate resulting in coffee ring.

Given that SERS is now a well established method for studying biomarkers [23], the motivation here is to establish the method further by improve throughput of SERS spectrum of biomarkers using the coffee ring formation. The biomarkers of interest are exosomes. Therefore, we prepared biological-simulated sample solution consisting of polystyrene beads (PS) and Phosphate Buffered Saline (PBS). PS diameter and density is almost same as biomarkers such as exosome, so PS can substitute for biomarkers [24]. Finally, we found that biological sample is separated into biomarkers and salt precipitation by LASER radiation for the biological sample droplet on the SERS substrate in the droplet evaporation progress, eventually this method improves the throughput of SERS spectrum of biomarker. This study will provide a widely implementable method in SERS and biology.

2. Materials AND METHODS

2.1 Sample preparation

Au nanopyramid substrate as SERS substrate is fabricated referring the reference paper[12],[22] and the image by SEM of our substrate is shown in Figure 2. The

pyramid base is 296 μm square on average. The height is 207 μm (The angle of the sidewalls of the pyramids relative to their basal plane is 57.5°, determined using crystallography of the Si crystal. [12])

Au flat substrate is fabricated by Au sputtering on Si substrate. Si wafer is purchased. Polystyrene beads (PS) in Milli-Q water is purchased from Alpha Nanotech Inc. The diameter is 100 nm, the content is 10 mg/mL, density is 1.05 g/mL. Calculating based on the specification, the original concentration is $1.8 \cdot 10^{13}$ particles/ mL. Phosphate Buffered Saline (PBS) is purchased from SIGMA-ALDRICH. The ingredients and concentration is shown in Table 1. Fluorescent polystyrene beads (fluorescent PS) is purchased from SIGMA-ALDRICH. The diameter is 500 nm, the content is 2.5%, density is 1.05 g/mL. Calculating based on the specification, the original concentration is $3.6 \cdot 10^{11}$ particles/ mL. Then it is diluted x1000 with PBS for fluorescent image experiment, so the final concentration is $3.6 \cdot 10^{8}$ particles/ mL. We prepared biological-simulated sample solution consisting of PS in PBS or DI water shown in

Table 2. It is known that concentration of exosome in the biological sample is almost 10^{8} particles/ mL, so our biological-simulated sample solution is considered reasonable.
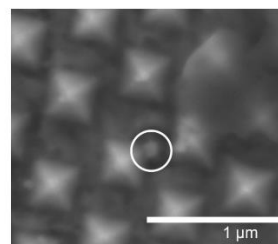

Figure 2 SEM image of the SERS Au pyramid substrate showing exosome

Table 1

Reagent	Amount, g	Concentration, mM
NaCl	8	137
KCl	0.2	2.7
Na$_2$HPO$_4$	1.44	10
KH$_2$HPO$_4$	0.24	1.8

Table 2

PS concentration, particles/ mL	Solution
$1.8 \cdot 10^{13}$	DI
$1.8 \cdot 10^{11}$	DI or PBS
$1.8 \cdot 10^{8}$	DI or PBS
0	DI or PBS

2.2 Taking video of droplet evaporation

We took the video of droplet evaporation process as shown Figure 3. The droplet volume is 3 μL The substrate is

Au nanopyramid substrate. The environment is the room condition. Every solution for this experiment is shown in Table 2.

2.3 Contact angle measurement polystyrene beads

We measured contact angle of the droplets. The droplet kinds and volume, substrate, experimental conditions are the same as in chapter 2.2. The contact angle is measured in the whole process from initial condition to evaporation perfectly.

2.4 Droplet evaporation under laser radiation

2.4.1 Some kinds of droplet evaporation under laser radiation

We irradiate the droplets on Au pyramid substrate with LASER. The droplet volume is 3 µL. The droplets are PBS solution containing PS of 10^8 particles/mL, DI water containing PS solution 10^8 particles/mL, and pure PBS. LASER is 785 nm wavelength, and the intensity is 103 mW.

2.4.2 Droplet evaporation under laser radiation on different kinds of substrate

To confirm whether the Au nanopyramid substrate has effect on the droplet evaporation phenomenon, we prepared Au flat substrate and Si wafer, then we irradiate the droplets on each substrate with LASER. The droplet volume is 3 µL. The droplets are PBS solution containing PS of 10^8 particles/mL. LASER is 785 nm wavelength, and the intensity is 103 mW.

2.4.3 Droplet evaporation under 3 wavelength laser radiation in the same intensity

To confirm whether changing LASER wavelength results in different evaporation phenomenon, we set up 3 wavelength 488, 633, 785nm LASER and irradiate the droplet with each wavelength LASER. The droplet volume is 3 µL. The droplet is PBS containing PS of 10^8 particles/mL. The intensity of every LASER is modified to close so that we can see the result differences due to LASER wavelength. The intensity of 785 nm LASER is 5.15 mW. The intensity of 633 nm LASER is 4 mW. The intensity of 785 nm LASER is 5.5 mW. The substrate is Au pyramid substrate.

2.5 Plasmonic simulation with FDTD

To discuss about the experiment in 2.4.2, we simulated the plasmonic effect with FDTD. The wavelength of light source is 488, 633 and 785 nm. The refractive index of the environment should be the same as water, so water refractive index $n(\lambda, t)$ ($t = 20\,°C = 293$ K) is calculated from the equation (2)[26][16]. The substrate material is Au and geometry is the same as Au nanopyramid substrate[1]. The base of nanopyramid is estimated to be 200nm square and the height is 140nm, the interval of pyramid apex is 400 nm.

$$n(\lambda, t) = A(t) + \frac{B(t)}{\lambda^2} + \frac{C(t)}{\lambda^4} + \frac{D(t)}{\lambda^6} \qquad (2)$$

$$A(293) = 1.32, B(293) = 5190, C(293) = -2.56 \times 10^8, D(293) = 9.39$$

2.6 Fluorescent image

We took fluorescent microscope image of droplet deposition after evaporation as shown in Figure 11. The droplet contains fluorescent polystyrene in PBS buffer. We made two droplet deposition. One is droplet which evaporated in the room condition and the other one is droplet which evaporated in LASER radiation. Both droplet volume is 3 µL. The droplet is PBS containing fluorescent PS. The concentration is $3.6 \cdot 10^8$ particles/ mL.

2.7. Raman mapping for the fluorescent image area

To establish to source of the bright spots, we did Raman measurement for the droplet deposition after evaporation to get Raman spectrum. The droplet deposition was prepared according to section 2.6 and Raman measurements points are in the area where fluorescent image is taken. To get enough Raman spectrum data, we got Raman signals by shifting the points by 5 µm. After getting the spectrum row data, we picked 1000 cm^{-1} intensity which is Polystyrene's most characteristic peak. Then we specifically plotted a 2D intensity map of the 1000 cm^{-1} peak. Regarding acquisition conditions, Raman LASER wavelength is 785 nm, the intensity is 10.3 mW, radiation time is 0.5 s. Then, we overlapped the Raman mapping on fluorescent image to confirm the relationship between the bright spots in the fluorescent images and 1000 cm^{-1} Raman intensity of PS.

3. Result

3.1 Observation of evaporation process

Shown in Figure 3, PS solution regardless in DI water or PBS, they finally formed coffee ring. Paying attention to the last-minute evaporation process of PBS solution containing PS, salt crystallization can be seen at first on the edge in Figure 3 (a). It can be explained by coffee ring effect. Then, we saw the crystallization on the center on the droplet in Figure 3(b). Finally, entire droplet evaporation starts at the area where there is no crystal between the center and edge towards the center and edge[25] while dendrite forming on the dried-up area. In addition, we can see the dendrite in the entire evaporation in Figure 3(c). The same last-minute evaporation process was seen in pure PBS evaporation. On the other hand, we can see different last-minute evaporation process in DI water containing polystyrene beads. Entire droplet evaporation starts at the edge of the droplet in Figure 4 (a) towards to the center in Figure 4 (b).
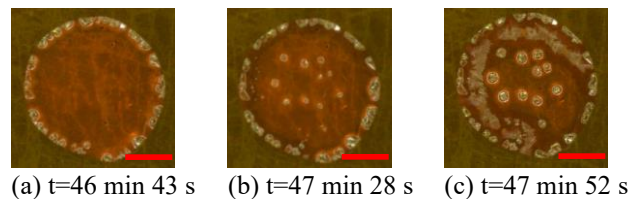

(a) t=46 min 43 s (b) t=47 min 28 s (c) t=47 min 52 s

Figure 3 Evaporation process of PBS droplet containing PS

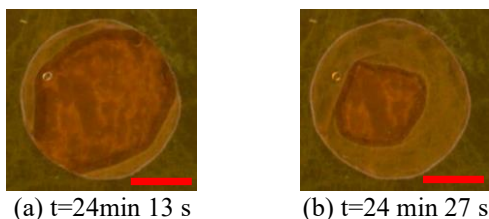The scale bar 1 mm. The PS concentration:1.8×10^8 particles/mL. Droplet volume is 3 μL.

| (a) t=24min 13 s | (b) t=24 min 27 s |

Figure 4 Evaporation process of DI water droplet containing PS

The scale bar 1 mm. The PS concentration:1.8×10^{11} particles/mL. Droplet volume is 3 μL.

3.2 Contact angle measurements

We can see that contact area of droplet and substrate starts shrinking (pinning effect ends) in early stage (t=500s) as to DI water in Figure 5 (a). Contrary, PBS shows long lasting pinning effect until 1700s in Figure 5 (b). Adding PS into DI, pinning effect last longer than DI and shows lower receding angle Figure 5 (c). Figure 5 (d) shows that adding PS into PBS makes less difference comparing to PBS regarding receding angle and pinning effect remaining time. Finally, we expressed the receding angle of each droplet in Figure 6. It shows that (1) containing PS shows lower receding contact angle in DI water. (2) containing PS shows less receding contact angle difference in PBS. (3) PBS containing PS shows lower receding angle than water containing the same concentration of PS. It indicates that ingredients consisting of PBS such as NaCl contribute to pinning effect a lot.
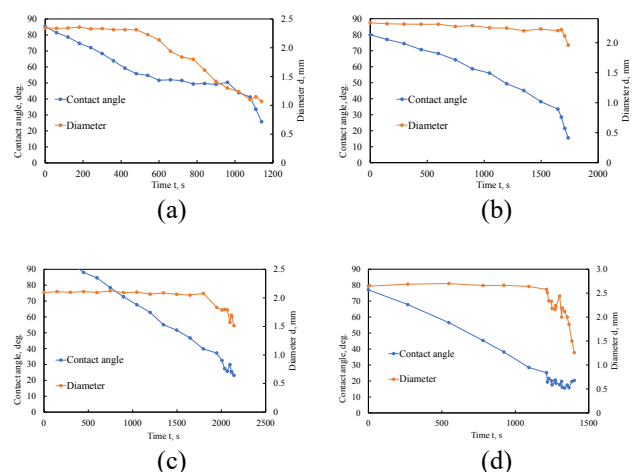
Figure 5 Contact angle measurements

(a) DI water (b)PBS (c) DI water containing PS whose concentration is $1.8 \cdot 10^8$ particles/mL (d) PBS containing PS whose concentration is $1.8 \cdot 10^8$ particles/mL
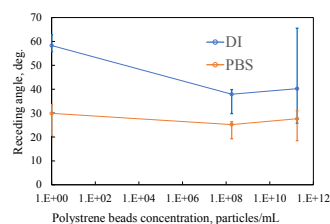

Figure 6 Receding angle

3.3 Droplet evaporation under laser radiation

Shown in Figure 7 (a), the biggest crystal can be seen at the LASER radiation point in PBS containing PS whose concentration is $1.8 \cdot 10^8$ particles/mL. On the other hand, PS would have been influenced by LASER radiation point, but Most of PS formed coffee ring in Figure 7 (b). Shown in Figure 7 (c), the biggest crystal can be seen at the LASER radiation point in PBS like Figure 7 (a). Comparing Figure 7 (a) and (c), pure PBS formed big precipitation and less coffee ring. A useful indication here is that Salt and PS deposit separately. By law of conservation of mass, if the precipitate size is large at the laser spot location, then there must be fewer salt precipitations elsewhere. Furthermore, since the polystyrene and salt deposit separately, this could help improve the throughput of SERS, because it addresses a key challenge mentioned previously.

Shown in Figure 8(a), (b), LASER irradiation effect is not confirmed with Au flat substrate and Si substrate. It indicates that Au nanopyramid substrate contributed to LASAR induced salt precipitation result.
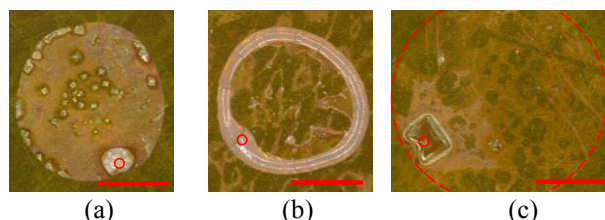

| (a) | (b) | (c) |

Figure 7 Various kinds of droplet evaporation under laser radiation LASER wavelength:785 nm

The scale bar 1 mm. The red circle indicates LASER spot. The red dashed circle indicates initial droplet size. LASER intensity is 103 mW (a) PBS containing PS whose concentration is $1.8 \cdot 10^8$ particles/mL (b) DI water containing PS whose concentration is $1.8 \cdot 10^{13}$ particles/mL (c) PBS
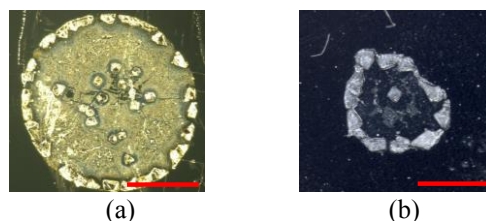

| (a) | (b) |

Figure 8 Droplet evaporation under laser radiation on kinds of substrate

The scale bar 1 mm. LASER wavelength:785 nm, LASER intensity:103 mW. Droplet is PBS containing PS whose concentration is $1.8 \cdot 10^8$ particles/mL (a) Au flat substrate (b) Si substrate
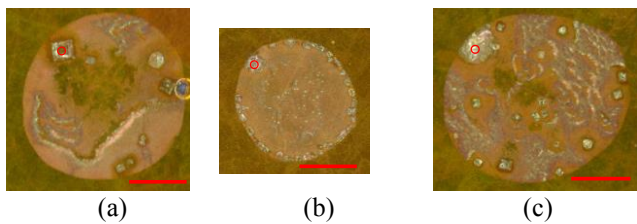
(a)   (b)   (c)

Figure 9 Droplet evaporation under 3 wavelength laser radiation

Droplet: PBS containing PS whose concentration is $1.8 \cdot 10^8$ particles/mL (a) 785 nm LASER. intensity is 5.15 mW (b) 633 nm LASER. intensity is 4 mW (c) 488 nm LASER. intensity is 5.5 mW

3.4 Plasmonic simulation

Results of FDTD simulation is shown in Figure 10 (a)-(c). 633 nm LASER enhanced electric field to 12 times at maximum and it's the best among 3 different wavelength LASER in Figure 10.
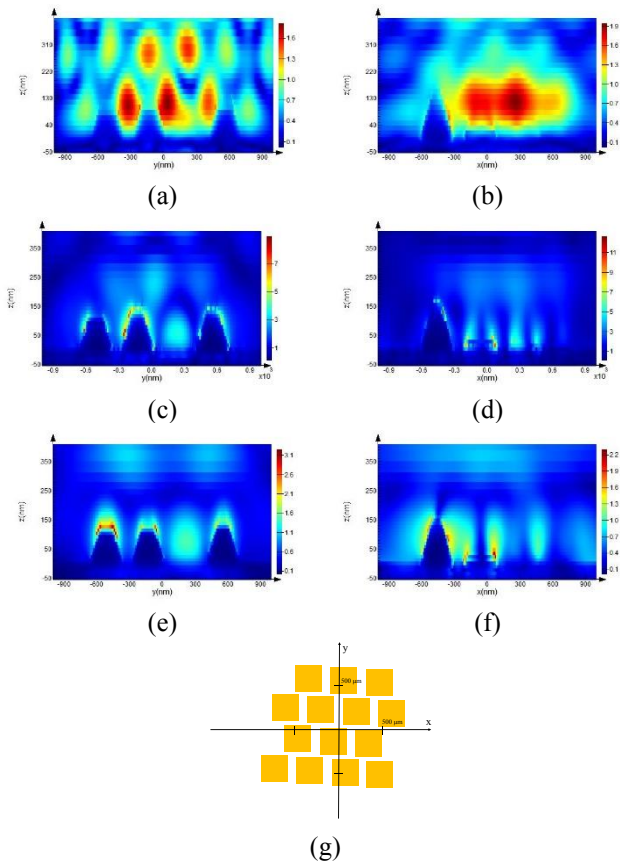

(a)   (b)

(c)   (d)

(e)   (f)

(g)

Figure 10 Plasmonic simulation with FDTD

(a) 785 nm LASER, x=0. (b) 785 nm LASER, y=0. (c) 633 nm LASER., x=0. (d) 633 nm LASER, y=0. (e) 488 nm LASER, x=0. (f) 488 nm LASER, y=0. (g) schematics of Au pyramid x-y coordinate. (z=0)

3.5 Fluorescent image

To validate that the PS beads indeed deposit separately from the salt, we the fluorescent imaging of dried up samples with fluorescent-PS beads was carrier out. The sample droplet

is fluorescent polystyrene in PBS buffer. We got fluorescent image shown in Figure 11 (a)-(c). Comparing with Figure 11 (d), (e), we can see the fluorescent light on the droplet deposition. Especially, we can see the brightest ring along the droplet edge. Contrary, we cannot see the fluorescent light on crystal area.
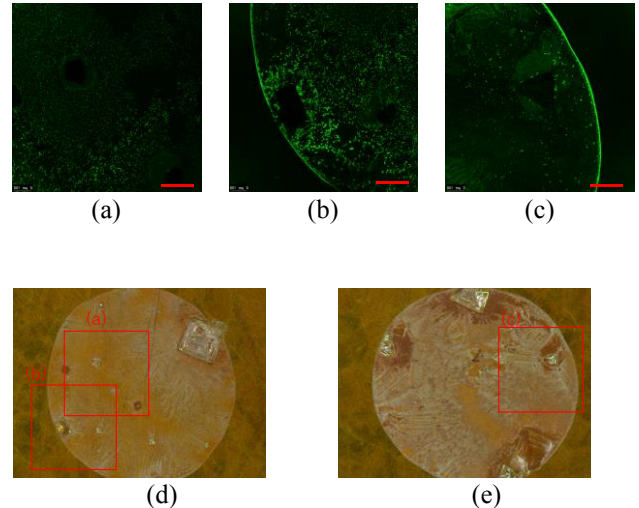

(a)   (b)   (c)

(d)   (e)

Figure 11 Fluorescent image of droplet deposition

The scale bar 200 μm. (a), (b) LASER irradiated sample. (c) without LASER irradiated sample.

(d), (e)microscope image showing the fluorescent image place. The fluorescent image size is 1.16 mm square.

3.5 Raman mapping

We need to prove that the green spots in fluorescent images are indeed the Polystyrene beads. We did Raman measurement for the droplet deposition after evaporation made in 2.6. The droplet consists of fluorescent polystyrene beads in PBS buffer. Raman Mapping was done at the locations where we obtained the fluorescent images. A location was selection in the middle of the droplet (figure 12 (c), (d)) and edge of droplet (figure 12 (e),(f)). Polystyrene exhibits a raman peak at 1000 cm^{-1}. A 2D colormap representing the height of 1000 cm^{-1} peak was plotted, as shown in figure 12 (d) and (f). As we can see Figure 12 (b) and (d), Figure 12 (e) and (f), there is a definite overlap of the mapping of the Polystyrene Raman peaks and the fluorescent image of the sample. This indicates that the green spots in fluorescent images are indeed polystyrene. Which means that the polystyrene is deposited separately from the salt crystals. Furthermore, We observe that the bead density is higher near the edges, thanks to the coffee ring effect.
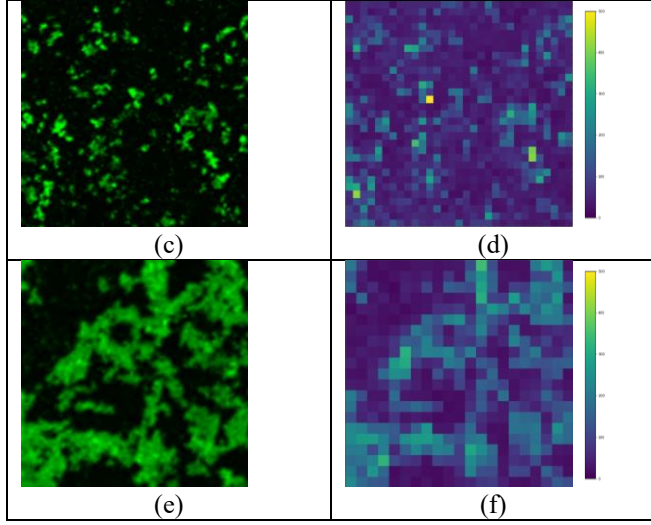

(a)   (b)
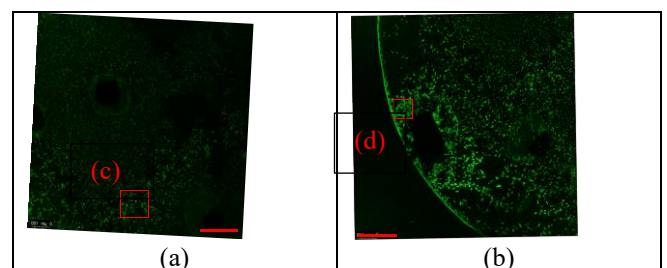
Figure 12 Fluorescent image and Raman mapping in the same location

(a) Fluorescent image the same as Figure 11 (a). The scale bar 200 μm. (b) Fluorescent image the same as Figure 11 (b). The scale bar 200 μm. (c) Fluorescent image indicated in Figure 12 (a). The image size is 150 μm. (d) Raman mapping conducted in Figure 12 (c). (e) Fluorescent image indicated in Figure 12 (b). The image size is 100 μm. (f) Raman mapping conducted in Figure 12 (e).

4. Discussion

We can see the dendrite in the entire evaporation in Figure 3(c). Dendrites are thought to have formed because the rapid drying rate exceeded the crystal growth rate of the salt.

From Figure 5 and Figure 6, salt precipitation derived from PBS increase the pinning force, which means salt precipitation has strong droplet retention. The results coincides that the entirely droplet evaporation starts at the point where salt crystal doesn't exist, then progress towards the salt crystal.

From Figure 7 and Figure 8, we see that the localized salt precipitation is observed on the Au-nanopyramid samples, and not on the flat-Au and Si samples. It can be considered that it is not just the LASER radiation, but the plasmonic effect which impacts salt crystallization. According to the reference papers, crystallization such as KCl starts on LASER radiation point and it's trapped by LASER[27]-[29]. These papers explains that the required free energy transforming ion clusters to nucleation become lower under electric filed and trapping force occurs under electric filed as well. This equation is expressed as equation (3), (4). The square of the electric field contributes to the free energy and trapping force. AS shown in Figure 10 Plasmonic simulation with FDTD plasmonic simulation by FDTD proved that our Au pyramid substrate improve the electric field. Therefore, only when using Au pyramid substrate, we saw the salt crystallization.

$$\Delta G(r, E) = 4\pi r^2 \gamma - \frac{4}{3}\pi r^3 (A\ln S + aE^2) \tag{3}$$

$$U_{trap} = \frac{1}{2}\alpha E^2 \tag{4}$$

To consider the effect of different wavelengths LASER on droplet evaporation we did experiments shown in Figure 9 and Figure 10. As a result, every LASER made salt crystal as shown in Figure 9. On the other hand, 633 nm LASER enhanced electric field the best in Figure 10 and it has the influence of the square of the electric field on salt crystallization. from equation (2), (3). However, we can see little difference among Figure 9(a)-(c). This is thought to be because the influence of the electric field is applied only to the area irradiated by the LASER and LASER spot size was 10μm diameter.

From Figure 12, we can see the positive correlation between fluorescent brightness and PS Raman peak mapping. The Raman mapping of the PS beads followed an identical areal pattern as the fluorophores observed in the fluorescent microscopy. Therefore, we can say that fluorescent image surely indicates the PS distribution. From Figure 11, we can see the brightest ring along the droplet edge. It's caused by coffee ring effect[13]. On the other hand, we cannot see the fluorescent brightness on the area crystal forms. We believe that PS were pushed out on the process of salt crystal growing, i.e. the coffee ring effect. In other words, the laser-assisted precipitation process primarily localizes the salt precipitation, and not the PS agglomeration. Hence, PS deposits separately. Further, conservation of mass would imply that since salt precipitation is localized, the amount of salt available for crystal and dendrite formation in other regions of the sample would reduce. Hence, the localized plasmonic precipitation also helps reduce the dendrite formation. This would help improve the throughput of the SERS spectrum.

5. Conclusion

- Salt crystallization starts at the edge of the droplet, then starts on the centre. Finally, entirely evaporation starts on the area where crystal doesn't exist, then progress towards the crystal while forming dendrite due to so high-speed evaporation that crystallization can't form.

- LASER radiation drying up method induced salt crystallization deriving from PBS. This can be explained that plasmonic effect caused by LASER and Au pyramid decreased the the required free energy transforming ion clusters to nucleation.

- From fluorescent image, PS doesn't exist on or inside the salt crystal. In other words, PS distribute on the area where salt doesn't form crystals. At the same time, the area is thought that dendrite can form.

- SERS throughput will be improved by LASER drying up method salt crystallization can be concentrated around the laser spot, which means the overall surface area of salt precipitation which hampers SERS of biomarker will decrease.

References

[1] Van der Pol, Edwin, et al. "Classification, functions, and clinical relevance of extracellular vesicles." Pharmacological reviews 64.3 (2012): 676-705.

[2] Taylor, Douglas D., and Cicek Gercel-Taylor. "MicroRNA signatures of tumor-derived exosomes as diagnostic biomarkers of ovarian cancer." Gynecologic oncology 110.1 (2008): 13-21.

[3] Vlassov, Alexander V., et al. "Exosomes: current knowledge of their composition, biological functions, and diagnostic and therapeutic potentials." Biochimica et Biophysica Acta (BBA)-General Subjects 1820.7 (2012): 940-948.

[4] Simpson, Richard J., et al. "Exosomes: proteomic insights and diagnostic potential." Expert review of proteomics 6.3 (2009): 267-283.

[5] Rabinowits, Guilherme, et al. "Exosomal microRNA: a diagnostic marker for lung cancer." Clinical lung cancer 10.1 (2009): 42-46.

[6] Michael, Amanda, et al. "Exosomes from human saliva as a source of microRNA biomarkers." Oral diseases 16.1 (2010): 34-38.

[7] Notingher, Ioan. "Raman spectroscopy cell-based biosensors." sensors 7.8 (2007): 1343-1358.

[8] Stiles, Paul L., et al. "Surface-enhanced Raman spectroscopy." Annu. Rev. Anal. Chem. 1 (2008): 601-626.

[9] Garrell, Robin L. "Surface-enhanced Raman spectroscopy." Analytical Chemistry 61.6 (1989): 401A-411A.

[10] Yan, Zhongbo, et al. "Self‐Aligned Trapping and Detecting Molecules Using a Plasmonic Tweezer with an Integrated Electrostatic Cell." Advanced Optical Materials 5.5 (2017): 1600329.

[11] Moskovits, Martin. "Surface‐enhanced Raman spectroscopy: a brief retrospective." Journal of Raman Spectroscopy: An International Journal for Original Work in all Aspects of Raman Spectroscopy, Including Higher Order Processes, and also Brillouin and Rayleigh Scattering 36.6‐7 (2005): 485-496.

[12] Yan, Zhongbo, et al. "A label-free platform for identification of exosomes from different sources."ACS sensors 4.2 (2019): 488-497. Buha, J., Lumley, R. N. & Crosky, A. G. Secondary ageing in an aluminium alloy 7050. Mater. Sci. Eng. A 492, 1–10 (2008).

[13] Deegan, Robert D., et al. "Capillary flow as the cause of ring stains from dried liquid drops."*Nature* 389.6653 (1997): 827-829.

[14] Boruvka, L., and A. W. Neumann. "Generalization of the classical theory of capillarity." The Journal of Chemical Physics 66.12 (1977): 5464-5476.

[15] Joanny, J. F., and Pierre-Gilles De Gennes. "A model for contact angle hysteresis." The journal of chemical physics 81.1 (1984): 552-562.

[16] De Gennes, Pierre-Gilles. "Wetting: statics and dynamics." Reviews of modern physics 57.3 (1985): 827.

[17] Hu, Hua, and Ronald G. Larson. "Evaporation of a sessile droplet on a substrate." The Journal of Physical Chemistry B 106.6 (2002): 1334-1344.

[18] Cazabat, Anne-Marie, and Geoffroy Guena. "Evaporation of macroscopic sessile droplets." Soft Matter 6.12 (2010): 2591-2612.

[19] Hu, Hua, and Ronald G. Larson. "Marangoni effect reverses coffee-ring depositions." The Journal of Physical Chemistry B 110.14 (2006): 7090-7094.

[20] Li, Yaxing, et al. "Evaporation-triggered segregation of sessile binary droplets." Physical review letters 120.22 (2018): 224501.

[21] Eales, Adam D., et al. "Evaporation of pinned droplets containing polymer–an examination of the important groups controlling final shape." AIChE Journal 61.5 (2015): 1759-1767.

[22] Xia, Ming, et al. "Coupling SPP with LSPR for enhanced field confinement: A simulation study. ”*The Journal of Physical Chemistry C* 120.1 (2016): 527-533.

[23] Choi, Namhyun, et al. "SERS biosensors for ultrasensitive detection of multiple biomarkers expressed in cancer cells." Biosensors and Bioelectronics 164 (2020): 112326.

[24] Wong, Tak-Sing, et al. "Nanochromatography driven by the coffee ring effect." Analytical chemistry 83.6 (2011): 1871-1873.

[25] Chen, Guofang, and Gideon J Mohamed. "Complex protein patterns formation via salt-induced self-assembly and droplet evaporation." The European Physical Journal E 33.1 (2010): 19-26.

[26] Bashkatov, Alexey N., and Elina A. Genina. "Water refractive index in dependence on temperature and wavelength: a simple approximation." Saratov Fall Meeting 2002: Optical Technologies in Biophysics and Medicine IV. Vol. 5068. SPIE, 2003.

[27] Ward, Martin R., and Andrew J. Alexander. "Nonphotochemical laser-induced nucleation of potassium halides: Effects of wavelength and temperature." Crystal growth & design 12.9 (2012): 4554-4561.

[28] Cheng, An-Chieh, Hiroshi Masuhara, and Teruki Sugiyama. "Evolving crystal morphology of potassium chloride controlled by optical trapping." *The Journal of Physical Chemistry C* 124.12 (2020): 6913-6921.

[29] Alexander, Andrew J., and Philip J. Camp. "Single pulse, single crystal laser-induced nucleation of potassium chloride." *Crystal Growth and Design* 9.2 (2009): 958-963.

JUACEP Workshop August 26th, 2022

Bio-sample droplet evaporation with LASER irradiation to induce salt precipitation aside and improve SERS throughput

Yusuke Terai

University of California, Los Angeles
Materials science and Engineering
Visiting Graduate Researcher
Supervisor: Prof. Ya-Hong Xie

Introduction-Exosome

Exosome [1]

Diameter = 30 - 200 nm
Containing nucleic acids and proteins

Cell
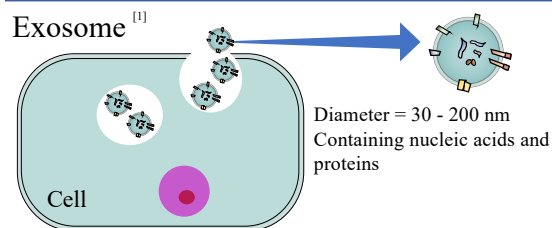
Role in spreading of diseases throughout the affected tissue

valuable source of biomarkers for diagnosing various diseases

[1]Vlassov, Alexander V., et al. "Exosomes: current knowledge of their composition, biological functions, and diagnostic and therapeutic potentials." Biochimica et Biophysica Acta (BBA)-General Subjects 1820.7 (2012): 940-948.

1/18

Introduction-Raman Spectroscopy

Raman Spectroscopy

detection

Lens

LASER

Raman scattered light

Sample

✓ Non-destructive
✓ chemical bonding in molecules

Available for biomarker, exosome
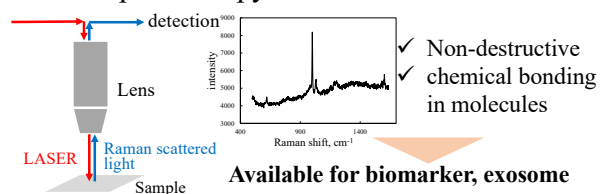
Surface-Enhanced Raman Spectroscopy (SERS)
with nanostructured metallic surfaces, Raman signals become much higher due to plasmonic effect

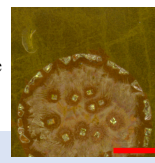2/18

Background

SERS for bio-sample

Biological sample

disease secreted exosomes

RNA Peak
Antigen & membrane protein Peak

Health exosomes

Exosomes Nano-Pyramid
SERS Measurement
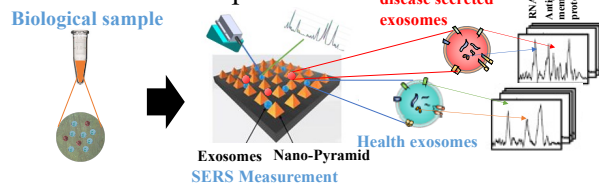
However
Biological sample includes exosome and salt
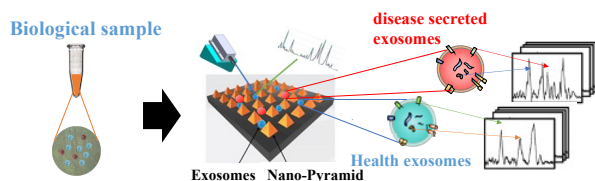
Problem
Salt precipitation disturb SERS signal of exosome

1mm

3/18

Objective

Establishing the method to improve throughput of SERS spectrum of exosome

Biological sample

disease secreted exosomes

Health exosomes

Exosomes Nano-Pyramid

4/18

Presentation topics

1. Introduction of sample
2. New method to control the precipitation in droplet evaporation.
3. Evaluation of new method

5

Sample

1. PBS phosphate buffered saline
2. Polystyrene beads diameter 100 nm
3. Au nano-pyramid substrate

6/18

Sample

1. PBS (phosphate buffered saline)

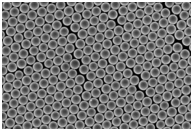| Reagent	Amount, g	Concentration, mM
NaCl	8	137
KCl	0.2	2.7
Na_2HPO_4	1.44	10
KH_2PO_4	0.24	1.8

7/18

Sample

2. Polystyrene beads diameter 100 nm

Exosome
Diameter = 30 - 200 nm
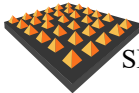
Polystyrene concentration, particles/ mL	Solution
1.8×10^{11}	DI
1.8×10^{8}	PBS
0	PBS

Almost the same concentration as exosome in bio-sample

8/18
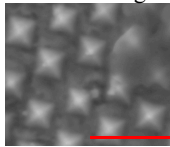
Sample

3. Au nano-pyramid substrate

SERS platform fabricated in the laboratory [4]

SEM image
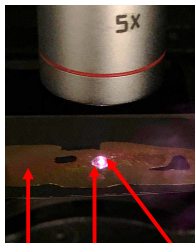

The Base is 296 nm square.
The height is 207 nm

1 µm

[4]Yan, Zhongbo, et al. "A label-free platform for identification of exosomes from different sources."ACS sensors 4.2 (2019): 488-497.
Buha, J., Lumley, R. N. & Crosky, A. G. Secondary ageing in an aluminium alloy 7050. Mater. Sci. Eng. A 492, 1–10 (2008). 9/18

Presentation topics

1. Introduction of sample
2. New method to control the precipitation in droplet evaporation.
3. Evaluation of new method

10

Droplet evaporation under LASER irradiation

Experiment conditions

LASER wavelength	785 nm
Intensity	108 mW
LASER spot size	1 µm

Droplet sample

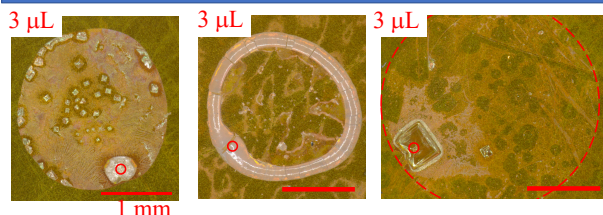| Polystyrene concentration, particles/ mL	Solution
1.8x1011	DI
1.8x108	PBS
0	PBS

Droplet   LASER irradiation
Au pyramid substrate

Hu, Hua, and Ronald G. Larson. "Evaporation of a sessile droplet on a substrate." The Journal of Physical Chemistry B 106.6 (2002): 1334-1344. 11/18

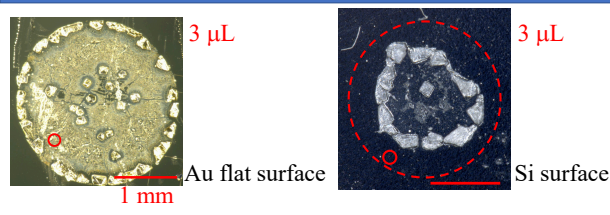## Droplet evaporation under LASER irradiation

3 μL   3 μL   3 μL

1 mm

Polystyrene in PBS
1.8×10^8 particles/mL

Polystyrene in DI water
1.8×10^{11} particles/mL

PBS

Salt crystallization can be seen at LASER radiation point on Au nano pyramid substrate.

12/18

Droplet evaporation under LASER radiation

3 μL

Au flat surface

3 μL

Si surface

1 mm

Polystyrene in PBS
1.8×10^8 particles/mL

Polystyrene in PBS
1.8×10^8 particles/mL

Salt crystallization cannot be seen at LASER radiation point on Au flat surface and Si surface.

Only gold pyramid substrate is effective for LASER irradiation method.
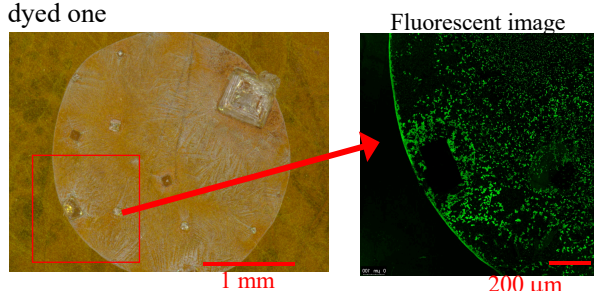
13/18

Presentation topics

1. Introduction of sample
2. New method to control the precipitation in droplet evaporation.
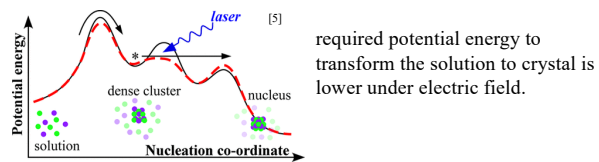3. Evaluation of new method

14

Fluorescent image

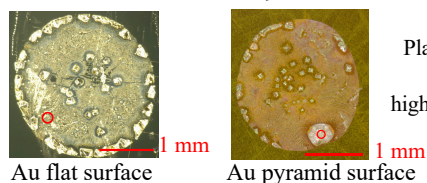Changing ordinal polystyrene beads to fluorescent dyed one

Fluorescent image

1 mm

200 μm

we cannot see the fluorescent brightness on the area crystal forms.

15/18

Discussion

laser [5]

required potential energy to transform the solution to crystal is lower under electric field.

Plasmonic effect

higher electric field

1 mm   1 mm

Au flat surface   Au pyramid surface

[5]Ward, Martin R., and Andrew J. Alexander. "Nonphotochemical laser-induced nucleation of potassium halides: Effects of wavelength and temperature." Crystal growth & design 12.9 (2012): 4554-4561.

16/18

Discussion

1 mm

200 μm
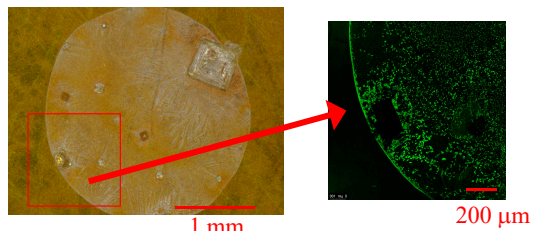
Salt crystal can be made on the side, which means the overall surface area of salt precipitation decrease.

Salt precipitation which disturbs SERS of exosome decrease.

SERS throughput will be improved by LASER drying up method

17/18

17

Conclusion

Conclusion

- ◆ Polystyrene beads distribute on the area where salt doesn't form crystals.
- ◆ Only on gold pyramid surface, salt crystallization by LASER can be seen.
- ◆ Plasmonic effect due to gold pyramid surface increased electric filed and the required potential energy to transform the solution to crystal decreased.

Future work

We need to confirm if the throughput of real
bio-sample improves with this method .

18/18

<2> Research Reports and Presentations

2-2. <u>2022 Medium-term course at Polytechnique Montréal</u>

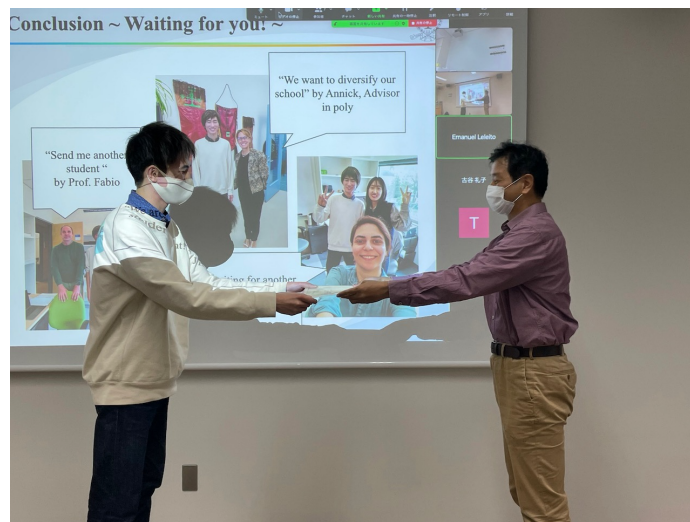### May 13, 2022 - September 6, 2022

Hirofumi Amada, *mentored by Prof. Fabio Cicoira, Chemical Engineering, Polytechnique Montréal*

[Research Report]
"Self-healing Property of PEDOT:PSS Film under High Humidity"
(Undisclosed) …P.21

[Presentation at the 28th JUACEP Workshop, October 6, 2022]
…P.22

SELF-HEALING PROPERTY OF PEDOT:PSS
FILM UNDER HIGH HUMIDITY

Hirofumi Amada

(Affiliation) Graduate School of Engineering, Nagoya University
amada.hirofumi.m0@s.mail.nagoya-u.ac.jp

Supervisor: Fabio Cicoira

(Affiliation) Department of Chemical Engineering, Graduate School of Engineering, Polytechnique Montreal
Fabio.cicoira@polymtl.ca

ABSTRACT

Poly (3,4-ethylenedioxythiophen) polystyrene sulfonate (PEDOT : PSS) is one of the most attractive materials because of its high stability, high electroconductivity, and self-healing property. Recently, water-enabled self-healing property [1] of PEDOT:PSS has attracted a great attention due to its novelty. However, the self-healing property under high humidity has not studied deeply yet. In this study, we focus on the self-healing property of PEDOT:PSS under high humidity. The sample of PEDOT:PSS film was made on a glass slide by drop-casting. Then, it was baked on a hot plate at 50 °C for 1 h, 90 °C for 1 h, and 140 °C for 4 h. After making the film, the sample was cut and divided into small samples ($1\ cm \times 3\ cm$). Finally, we measured the current of samples under high humidity and discovered how it behaves under several conditions.

Undisclosed

Final Presentation
Juacep Program

Polytechnique de Montreal, research intern student

Nagoya University, Graduate School of Engineering, Chemical Systems Engineering

Hirofumi Amada

Outline

1. Outline of research
2. Life in Montreal
   2.1 About Montreal
   2.2 Grocery and Food
   2.3 Housing and Rent
   2.4 School life in poly
   2.5 Activity and travel in another city!
   2.6 total cost
3. Conclusion

Outline

1. Outline of research
2. Life in Montreal
   2.1 About Montreal
   2.2 Grocery and Food
   2.3 Housing and Rent
   2.4 School life in poly
   2.5 Activity and travel in another city!
   2.6 total cost
3. Conclusion

---

1. Outline of research

✓ Welcome to Fabio Lab

Organic Electronics with Flexibility

1. Self-healable conducting polymers
2. Stretchable electronics
3. IN VIVO organic bioelectronics
4. Patterning and printing for flexible electronics
5. Metal oxide electronics
6. Mixed ionic electronic transport in organic devices
7. Carbon based electrodes for organic thin film transistors
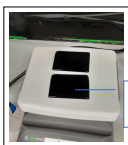
---
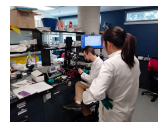
1. Outline of research

Research in poly

Will be published

Confidential

1. Self-healing project in Fabio lab
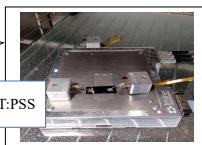2. Collaborative project with Philip Morris

1. Self-healing project under high humidity
※It will be published in paper⇒ I can't show them all.
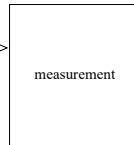
PEDOT:PSS

measurement

Baked on a hot plate   Make a gap and set it on a device

---

1. Outline of research

2. Collaborative project with Philip Morris
※ I can't show them all as well (confidential)

What is Philip Morris International?

✓ The biggest cigarette company in the world.
✓ famous product : Marlboro

PHILIP MORRIS INTERNATIONAL

Cigarette   Electric cigarette

✓ Organic Electronics & Cigarette Paper

21

Outline

Life in Montreal ~ About Montreal~

✓ When it comes to Montreal…

➢ Official language : French &French culture

➢ Nature & City

➢ Tourist & Business

➢ Technology & Art

Life in Montreal ~ Grocery and Food ~

✓ Food itself is cheap
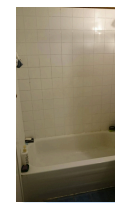
⇨

✓ Food with service is expensive

➢

$19.55

Life in Montreal ~ Housing and rent ~

✓ Housing is very expensive in Canada

✓ Expected cost for the living : $500 CAD

✓

DO NOT rent the house privately
⇨ Rent the dormitory!!!!
Otherwise you could be kicked out

Life in Montreal ~ School life in poly ~

Activity and travel in another city!

Life in Montreal ~ total cost ~

<Living expense / month>	<flight and insurance>
・rent : $500	・flight : $2000
・Food : $300	・Insurance : $1000
・metro pass : $50	for 4months
・Phone : $30	
・miscellaneous : $120	
Travel to Toronto : $500	Total : $ 7750
OSHEAGA : $100	Scholarship from poly
Quebec tour : $150	: $4000
	*No JASSO

13

Conclusion ~ Waiting for you! ~

"Send me another student " by Prof. Fabio

"We want to diversify our school" by Annick, Advisor in poly

"We are waiting for another student!!" by Sarah and Jinsil

14

⟨2⟩ Research Reports and Presentations

2-3. <u>2022 Medium-term course at UCLA</u>

August 30, 2022 - February 22, 2023

[Research Reports]

Kentaro Takagi*, mentored by Prof. Tetsuya Iwasaki, Mechanical and Aerospace Engineering,*
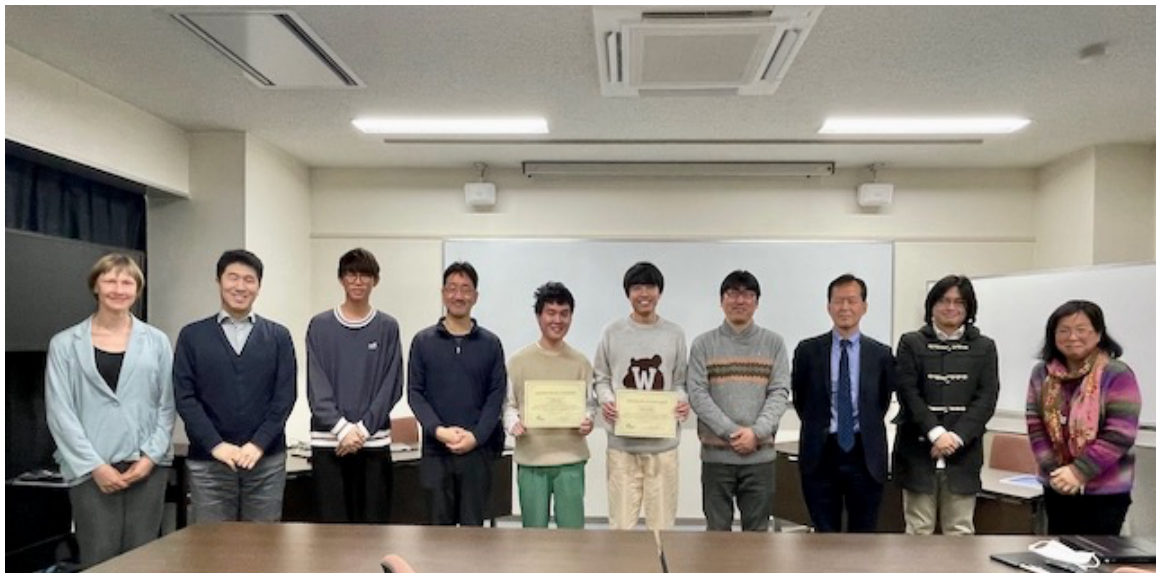"Identifying the Network of Bursting Neurons in CPG" …P.26

Hiroshi Goto*, mentored by Prof. Kang L. Wang, Electrical and Computer Engineering,*
"Observing the Chiral-Induced Spin Selectivity Effect"
(Undisclosed) …P.31

[Presentations at the 29th JUACEP Workshop, March 14, 2023]
…P.32

IDENTIFYING THE NETWORK OF BURSTING NEURONS IN CPG

Kentaro Takagi

Department of Mechanical Systems Engineering, Graduate School of Engineering, Nagoya University
takagi.kentaro.d4@s.mail.nagoya-u.ac.jp

Supervisor: Tetsuya Iwasaki

Department of Mechanical and Aerospace Engineering, University of California, Los Angeles
tiwasaki@ucla.edu

ABSTRACT

The central pattern generator (CPG) is a nonlinear oscillator formed by a group of neurons, providing a fundamental control mechanism underlying rhythmic movements in animal locomotion. We consider a class of CPGs modeled by a set of interconnected identical bursting neurons. Based on the idea of multivariable harmonic balance, we approximate oscillatory signal as a sinusoid and show the limitation of the harmonic balance for capturing the phase property. We propose a new method that directly find the connectivity matrix from the raw data.

1. INTRODUCTION

Rhythmic movements of animals, such as walking, breathing, and swimming are controlled by a neural network known as the central pattern generator (CPG). These neurons are interconnected in a specific manner and oscillate with phase relations, generating a pattern that activates the muscles. To understand how this biological control mechanism works, CPGs have been thoroughly studied in neuroscience research [1]. Researchers have identified individual neurons that participate in rhythmic pattern generation and have observed their connections through physiological experiments. Despite this, the observed connections are not precise enough and there is no systematic way that could specify the connections with greater precision without conducting the experiments, thus we will focus on bursting neuron model which closely approximates the biological properties and behavior of real neurons in the CPG.

The knowledge gained from studying CPGs has been applied in engineering, particularly in robotics, where the basic architectures of CPGs are used to design feedback controllers that achieve stable limit cycles with desired phase coordination properties [2]. Many literatures contain theoretical analysis methods for CPGs, but they are not useful for analysis and synthesis problem of designing CPGs to achieve oscillations with a desired profile (frequency, amplitudes, and phases). The analysis problem addressed in this report is to determine whether a stable oscillatory trajectory exists and, if so, to predict the oscillation profile. The synthesis problem is to determine appropriate neuronal connections so that the resulting CPG achieves a stable oscillation with a desired profile. The synthesis problem not only pertains to the design of artificial CPGs to regulate the locomotion systems of robots, but also pertains to the insight into neuronal mechanisms underlying the generation of specific oscillation patterns.

The systematic method using multivariable harmonic balance are used for analysis and synthesis of CPGs in literature [3]. The multivariable harmonic balance is a technique that can quantify the oscillation profile by approximating the oscillatory signal into a sinusoid. This multivariable harmonic balance approach has clarified that oscillation profile can be achieved from the eigenvector and the eigenvalue of neuronal connectivity matrix when the amplitudes are uniform.

The aim of this research is to identify a method that can solve the problems associated with designing CPGs using bursting neurons. The ultimate goal is to achieve advancements not only in engineering but also in the field of neuroscience.

2. BURSTING NEURON MODEL

The model we use is bursting neuron model. A bursting neuron is a type of neuron that exhibits a pattern of activity characterized by alternating periods of high-frequency spiking and periods of no spikes. A model for a single bursting neuron is based on Hodgkin-Huxley model and is given by [4]

$$c\dot{v} + I_{Na} + I_{NaP} + I_K + I_L + I_I = I_o, \tag{1}$$

$$n + \tau_n \dot{n} = n_\infty(v), \tag{2}$$

$$h + \tau_h \dot{h} = h_\infty(v), \tag{3}$$

$$g_x + \tau_x \dot{g}_x = \bar{g}_x u_x, \quad x := E, I, \tag{4}$$

where

$$I_x = g_x(v - E_x), x := Na, K, NaP, L, E, I, \tag{5}$$

$$g_{Na} = \bar{g}_{Na} m_\infty(v)^3 (1 - n), \tag{6}$$

$$g_K = \bar{g}_K n^4, \tag{7}$$

$$g_{NaP} = \bar{g}_{NaP} \mu_\infty(v) h, \tag{8}$$

$$g_L = \bar{g}_L, \tag{9}$$

$$x_\infty(v) = 1/(1 + e^z), z := (v - \theta_x)/\sigma_x, x := n, h, m, \mu \tag{10}$$

$$\tau_x = \bar{\tau}_x / \cosh(z/2), x := n, h \tag{11}$$

The semipermeable cell membrane separates the interior of the cell from the extracellular liquid and acts as a capacitor. The cell has ionic channels that have different batteries (mV) which are E_{NaP}, E_{NaP}, E_K, E_L. c is the whole cell capacitance and v is the membrane potential. I_{Na}, I_{NaP}, I_K, I_L are ionic currents and I_E, I_I are excitatory and inhibitory currents from another cell, respectively. g_{Na}, g_{NaP}, g_K, g_L, g_E, g_I are conductances (nS). n, m, h, μ are voltage-dependent (in)activation variables that regulate whether each ionic channel is open or not. τ_x is the voltage-dependent time constant and $x_\infty(v)$ is the steady-state voltage-dependent (in)activation function of x. τ_x is the voltage-dependent time constant (ms). When there are N neurons in a network, the synaptic excitatory/inhibitory input of i_{th} neuron u_{Ei}/u_{Ii} is given by the weighted sum of the presynaptic potentials:

$$u_{Ei} := b_{Ei} + \sum_{j=1}^{N} \phi(\omega_{ij}) \psi(v_j) \tag{12}$$

$$u_{Ii} := b_{Ii} - \sum_{j=1}^{N} \phi(-\omega_{ij}) \psi(v_j) \tag{13}$$

$$\phi(z) := \max(0, z), \psi(x) := \frac{\phi(x - v_{th})}{v_{max} - v_{th}}$$

where ω_{ij} is the coupling strength of the connection from neuron j to neuron i, which is positive/negative when the connection is excitatory/inhibitory, with its magnitude reflecting the strength. Note that, for an excitatory connection, $\omega_{ij} > 0$, $\phi(\omega_{ij}) = \omega_{ij}$ and $\phi(-\omega_{ij}) = 0$ for an inhibitory connection, $\omega_{ij} < 0$, $\phi(\omega_{ij}) = 0$ and $-\phi(-\omega_{ij}) = |\omega_{ij}|$, and for no connection, $\omega_{ij} = 0$. b_{Ei} and b_{Ii} are constant bias input. The parameter values are

$c = 21$ pF,

$\bar{g}_K = 11.2$, $E_K = -85$, $\theta_n = -29$, $\sigma_n = -4$, $\bar{\tau}_n = 10$,

$\bar{g}_{Na} = 28$, $E_{Na} = 50$, $\theta_m = -34$, $\sigma_m = -5$,

$\bar{g}_{NaP} = 2.8$, $E_{NaP} = 50$, $\theta_\mu = -40$, $\sigma_\mu = -6$,

$\bar{g}_L = 1.2$, $E_L = -65$, $\theta_h = -48$ mV, $\sigma_h = 6$ mV, $\bar{\tau}_h = 1000$.

We adjusted the value of $\bar{g}_L$ from 2.8 to 1.2 so that the model produces a self-bursting behavior with no inputs ($I_o = u_E = u_I = 0$). The value of $\bar{\tau}_h$ has been modified from 10000 to 1000 in order to shorten the bursting period. The synaptic channel currents are modeled in a standard way (exponentially decaying conductance after a presynaptic impulse), and the parameter values (except v_{th} and v_{max}) are set from [5] as

$b_E = 0$, $\bar{g}_E = 1.0$, $E_E = 0$, $\tau_E = 5$, $v_{th} = -40$,

$b_I = 0$, $\bar{g}_I = 1.0$, $E_I = -75$, $\tau_I = 15$, $v_{max} = 5$.

The value of the current injection I_o should be chosen appropriately for generating bursting oscillations. This effect can be equivalently captured by increasing E_L by $I_o/\bar{g}_L$. We simulate the neuron model by using ODE45 in MATLAB. A simulation result of self-bursting neuron is shown in Fig. 1, where the initial condition was,

$$x(0) = \text{col}(-64, 0.1, 0.9, 0, 0), x := \text{col}(v, n, h, g_E, g_I).$$
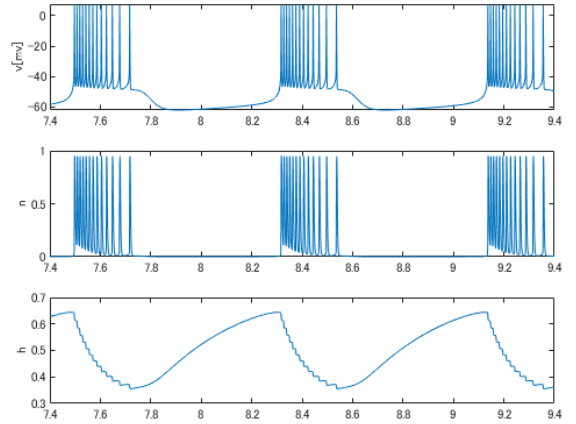
The bursting period is $T = 820$ [ms].

Figure 1. Self-bursting neuron

3. APPROACH

3.1 Harmonic balance

To solve the analysis and synthesis problem, we first applied the harmonic balance. The input and output of i_{th} neuron is defined as $u_i := u_{Ii}$ and $y_i = \psi(v_i)$, respectively. Both input and output are approximated by sinusoids using Fourier transform

$$u_i \cong u_i^s := \text{Im}[\hat{u}_i e^{i\omega t}] + \bar{u}_i \tag{14}$$

$$y_i \cong y_i^s := \text{Im}[\hat{y}_i e^{j\omega t}] + \bar{y}_i \tag{15}$$

where $\omega := 2\pi/T$ and T is bursting period. $\hat{u}_i$ and $\hat{y}_i$ are complex numbers indicating the phasors of u_i and y_i, respectively, whereas $\bar{u}_i$ and $\bar{y}_i$ are real numbers indicating the bias values. The frequency response (FR) of each neuron at ω is then defined by the bias gain $g_i := \bar{y}_i/\bar{u}_i$, harmonic

gain $f_i := \hat{y}_i/\hat{u}_i$, and phase $\arg(\hat{y}_i) - \arg(\hat{u}_i)$. Let F and G be the diagonal matrix that have f_i and g_i, respectively as diagonal elements, and let M be the connectivity matrix of a network. u can be denoted as

$$u = My + \beta \qquad (16)$$

Combining (16) with F and G, we get

$$\hat{u} = MF\hat{u} \qquad (17)$$

$$\bar{u} = MG\bar{u} + \beta \qquad (18)$$

The equations (17) and (18) imply that $\hat{u}$ and $\bar{u}$ are eigenvector of MF and MG with corresponding eigenvalue 1, provided $\beta = 0$. When u_i^s is given and if we know the frequency response of a single neuron under sinusoids with different amplitudes, we could predict F and G, and can find out M. However, this method is not going to work if resulting output is different with the actual output. Figure 2 shows the simulation result of matrix W_1, a recurrent cyclic inhibition oscillator (RCI), and Table 1 shows the frequency components.

$$W_1 = \begin{bmatrix} 0 & -3 & 0 \\ 0 & 0 & -3 \\ -3 & 0 & 0 \end{bmatrix}, T = 1108 \text{ ms}$$
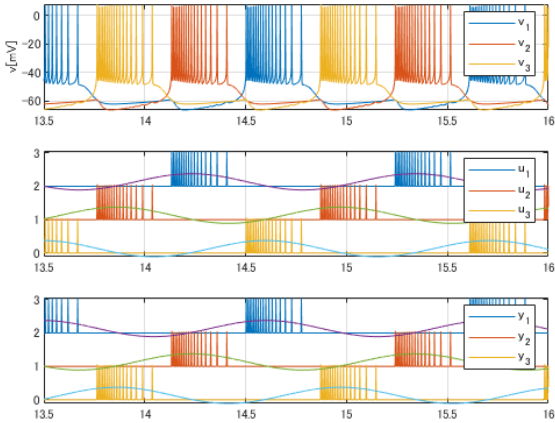

Figure 2. RCI oscillator

Table 1 Frequency components of RCI oscillator

	bias	amp	phase
u_1^s	0.0800	0.1453	178
y_1^s	0.0267	0.0484	-62
FR	0.3333	0.3333	-120
fr	0.3336	0.3355	-149
$\tilde{u}_1^s$	-0.005	0.1462	-120
$\widetilde{\text{fr}}$	-8.25	0.3174	-120

The fourth row of the table indicates the frequency response (fr) of the single neuron under input u_1^s. The output of the neuron for input u_i^s is denoted as y_i^s, and its sinusoidal approximation containing the bias and fundamental frequency components is represented as $\tilde{y}_i^s$. Then the bias gain, harmonic gain, and phase are determined

in a similar way to FR. The phase error in fr is found to be significant, indicating that u_i^s is not an accurate approximation of u_i. While adjusting the bias of u_i can result in a phase lag of $120°$, as observed in a simulation, it is not clear how to systematically adjust the bias.

Figure 3 shows the simulation result of matrix of W_2, RIO-plus. Table 2, 3, 4 show the frequency components of each neuron.

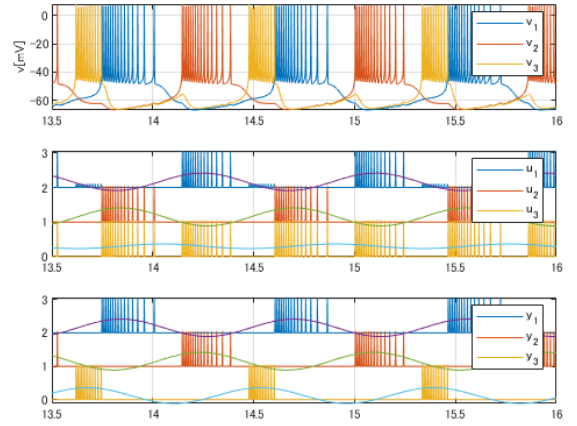$$W_2 = \begin{bmatrix} 0 & -3 & -0.3 \\ -3 & 0 & 0 \\ -3 & -3 & 0 \end{bmatrix}, T = 858 \text{ ms}$$

Figure 3. RIO-plus

Table 2 Frequency response of Neuron 1

	bias	amp	phase
u_1^s	0.0982	0.152	0
y_1^s	0.0302	0.0520	170
FR 1	0.308	0.344	170
fr 1	0.309	0.344	174

Table 3 Frequency response of Neuron 2

	bias	amp	phase
u_2^s	0.0906	0.156	170
y_2^s	0.0303	0.0531	4
FR 2	0.334	0.340	194
fr 2	0.334	0.346	175

Table 4 Frequency response of Neuron 3

	bias	amp	phase
u_3^s	0.181	0.0399	83
y_3^s	0.0246	0.0473	239
FR 3	0.136	1.18	156
fr 3	-	-	-

The amplitude of u_3^s is smaller than those of u_1^s and u_2^s. This is because u_3 is the weighted sum of y_1 and y_2, and the fundamental frequency component is much smaller than the second harmonic component with frequency 2ω, which has the amplitude 0.218. As a result, the response of the single neuron to u_3^s does not have a steady bursting (with period fluctuation). This example shows the limitation of the harmonic balance with the fundamental frequency component for capturing the phase coordination behaviors.

3.2 Network Modeling

The previous section suggests that it may be difficult to use the harmonic balance for modeling neuronal circuits since sinusoidal approximations do not always capture the phase property of a single neuron accurately. This section considers a more direct approach for modeling, where the raw data, rather than harmonic approximations, are used. The basic idea is to compute u and y , and then find out M from the equation (16), where membrane potential v is assumed given and $\beta = 0$.

We will develop a numerically tractable constraint equation for W so that the data and the model behavior are consistent. First note that the (estimated) ion channel current $I(t) := I_{Na} + I_K + I_{NaP} + I_L$ can be computed from $v(t)$ through numerical integration. The model is then described as

$$c\dot{v} + I + g_I(v - E_I) = 0 \qquad (19)$$

$$g_I = \frac{\bar{g}_I}{1 + \tau_I s} u, u = \phi(-W)\psi(v),$$

or equivalently,

$$c\frac{\dot{v}}{v - E_I} + \frac{I}{v - E_I} + g_I = 0. \qquad (20)$$

Note that

$$x := \log(v - E_I), \dot{x} = \frac{\dot{v}}{v - E_I}. \qquad (21)$$

Then we have

$$c\dot{x} + Ie^{-x} + g_I = 0. \qquad (22)$$

Adding $ax - ax$ on the left side with $a \ge 0$, and taking the Laplace form,

$$\chi := \frac{1}{a + cs}(ax - Ie^{-x}) - x = \frac{g_I}{a + cs} = \phi(-W)\eta \quad (23)$$

$$\eta := \frac{\bar{g}_I \psi(v)}{(a + cs)(1 + \tau_I s)} \qquad (24)$$

To compute χ without calculating $\dot{x}$, let y as

$$y := \frac{1}{a + cs}(ax - Ie^{-x}). \qquad (25)$$

χ is

$$\chi = y - x.$$

Differential equation of y is

$$\dot{y} = -\frac{a}{c}y + \frac{a}{c}x - \frac{I}{c}e^{-x}. \qquad (26)$$

χ is computable from $v(t)$ via simulation. From equation (24), differential equation of η is

$$\ddot{\eta} = \frac{-a\tau_I + c}{c\tau_I}\dot{\eta} - \frac{a}{c\tau_I}\eta + \frac{\bar{g}_I \psi(v)}{c\tau_I}. \qquad (27)$$

η is also computable from $v(t)$. The connectivity matrix can be found by solving $\chi = \phi(-W)\eta$. With $a = 0$, the values of $\chi(t)$ and $\eta(t)$ may be unbounded and hence this case is not suitable for computing W. With $a > 0$, however, both $\chi(t)$ and $\eta(t)$ are well defined (bounded) as periodic functions, which are suitable for computing W. To solve $\chi = M\eta$ ($M := \phi(-W)$) for M, extract one bursting period of time as $0 = t_0 < t_1 < t_2 < \cdots < t_n = T$. Then solve for M by using Moore-Penrose inverse of Y.

$$X = MY \to M = XY^\dagger \qquad (28)$$
$$, X := [\chi(t_1) \dots \chi(t_n)], Y := [\eta(t_1) \dots \eta(t_n)]$$

For RCI oscillator, calculated M is numerically comparable with the actual M.

4. CONCLUSION

We first applied the harmonic balance method to solve the problems associated with designing CPGs that use bursting neurons. By simulation, we verified the limitation of this method with the fundamental frequency component for capturing the phase coordination behaviors. For the alternative method, we proposed the modeling method to develop a numerically tractable constraint equation for W so that the data and the model behavior are consistent. This method avoids calculating $\dot{v}$ and unbounded integral of some signals. In future work, we are going to use the sinusoidal approximation of given v instead of v to calculate connectivity matrix. If this works, then the modeling may be done to reproduce the bursting behavior in terms of the bursting period and phase, possibly ignoring the details of the spiking frequency, which may be more practical.

REFERENCES

[1] Cohen, A., Rossignol, S., & Grillner, S. (1988). Neural control of rhythmic movements in vertebrates. Wiley-Interscience.

[2] Crepsi, A., Badertscher, A., Guignard, A., & Ijspeert, A. (2005). Amphibot I: An amphibious snake-like robot. Robotics and Autonomous Systems, 50, 163–175.

[3] Iwasaki, T. (2008). Multivariable harmonic balance for central pattern generators. Automatica, 44(12), 3061-3069.

[4] R.J. Butera, J. Rinzel, and J.C. Smith. Models of respiratory rhythm generation in the pre-bontzinger complex. I. bursting pacemaker neurons. J. Neurophys., 82(1):382–397, 1999.

[5] I.A. Rybak, A.P.L. Abdala, S.N. Markin, F.R. Paton, and J.C. Smith. Spatial organization and state- dependent mechanisms for respiratory rhythm and pattern generation. Prog. Brain Res., 165:201–220, 2007.

OBSERVING THE CHIRAL-INDUCED SPIN SELECTIVITY EFFECT

Hiroshi Goto

Department of Applied Physics, Graduate School of Engineering, Nagoya University
goto.hiroshi.u5@s.mail.nagoya-u.ac.jp

Kang L. Wang

Department of Electrical and Computer Engineering, University of California, Los Angeles
klwang@ucla.edu

ABSTRACT

Since the phenomenon that a direction of an electron's spin is selected by chiral molecules somehow while it is passing through chiral molecules 2 decades ago, it is expected that this effect is applied for spintronics devices. That is so-called "*chiral-induced spin selective* (CISS) *effect*" and some research show their spin polarization can exceed that of ferromagnets[1] despite those molecules consist of light elements. However, its origin has been under debate yet and it is important that fundamental mechanism is made clear as well as application. In this study, two kinds of experiments were conducted to observe the CISS effect with two kinds of chiral molecules with which that effect has already been observed in previous study[2].

Undisclosed

The 29th JUACEP Workshop

for the medium-term research course students from Nagoya University to UCLA

Date: Tuesday, March 14. 2023
Venue: Aerospace Meeting Room 347, 3rd floor Eng-Bldg 2

11:00

OPENING ADDRESS BY JUACEP LEADER

11:05 – 11:20

PRESENTER: KENTARO TAKAGI

ADVISOR: PROF. TETSUYA IWASAKI

MECHANICAL & AEROSPACE ENGINEERING, UCLA

11:20 - 11:35

PRESENTER: HIROSHI GOTO

ADVISOR: PROF. KANG L. WANG

ELECTRICAL & COMPUTER ENGINEERING, UCLA

11:40

COMPLETION CEREMONY

052-789-2799 JUACEP Office

Identifying the Network of Spiking Neurons in CPG

Kentaro Takagi

Background(1/2)

Spinal cord injury (SCI)

- disrupt the neural connections within the CPG which is located in the spinal cord

- result in walking difficulties

- there is no cure

- rehabilitation is available to manage symptoms and improve quality of life.

Neuron

CPG

After SCI…
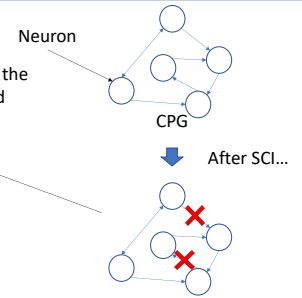
Background(2/2)

What is rehab in SCI?

- aim to reform connections within the CPG through neuroplasticity

- applying **electrical stimulation** is one way

Finding out appropriate frequency, intensity, phase timing, and location of such stimulation is needed

Objective

Identifying the network connection of biological CPG is needed to capture the effect of stimulation

CPG

After rehab…
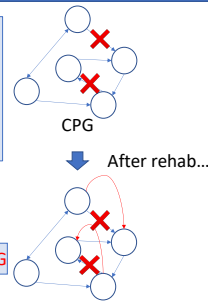
Spiking neuron model

Hodkin-Huxley model

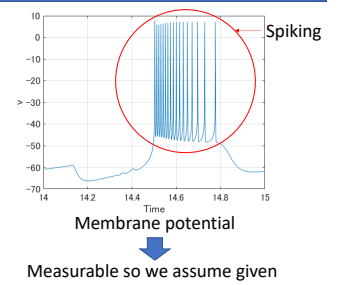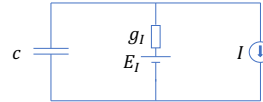$$c\dot{v} + I(v) + g_I(v - E_I) = 0$$
$$g_I + \tau_I \dot{g}_I = u$$
$$u = My \qquad y = \psi(v)$$

v: membrane potential
u: input $\quad \tau_I$: const
M: network connectivity matrix
ψ: nonlinear function

c $\quad$ g_I $\quad$ I
$\quad E_I$

Spiking

Membrane potential

Measurable so we assume given

Example

$$c\dot{v} + I(v) + g_I(v - E_I) = 0$$
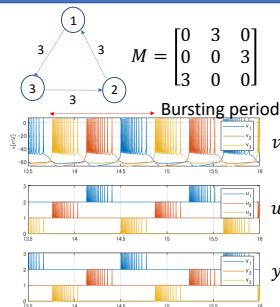$$g_I + \tau_I \dot{g}_I = u$$
$$u = My$$

v: membrane potential
u: input $\quad \tau_I$: const
M: network connectivity matrix
ψ: nonlinear function

Bursting is a steady state where a train of spikes are followed by a period of no spikes and this pattern repeats

$$M = \begin{bmatrix} 0 & 3 & 0 \\ 0 & 0 & 3 \\ 3 & 0 & 0 \end{bmatrix}$$

Bursting period

v

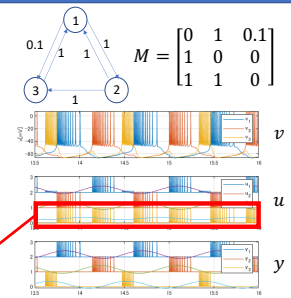u

y

1st Approach

Spiking neuron model
- nonlinear
- have steady state (bursting)

Approach: Harmonic Balance

A method applied to approximate periodic steady state solutions of nonlinear differential equations by a sinusoid

Would sinusoid be good approximation?

u_3 doesn't have steady bursting
→limitation of harmonic balance

$$M = \begin{bmatrix} 0 & 1 & 0.1 \\ 1 & 0 & 0 \\ 1 & 1 & 0 \end{bmatrix}$$

v

u

y

2ⁿᵈ Approach

Problem:
Given v, find M

$c\dot{v} + I(v) + g_I(v - E_I) = 0$
$g_I + \tau_I \dot{g}_I = u$
$u = M\psi(v)$

v contains noise
→$\dot{v}$ is more noisy

u is incomputable without M
→g_I is also incomputable

Solution:
Formulate equation that can find M without using g_I and $\dot{v}$
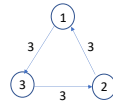
$$\chi = M\eta$$

$\chi = y - x$
$x = \log(v - E_I)$
$\dot{y} = -\frac{a}{c}y + \frac{a}{c}x - \frac{I}{c}e^{-x}$
$\ddot{\eta} = \frac{-a\tau_I + c}{c\tau_I}\dot{\eta} - \frac{a}{c\tau_I}\eta + \frac{\bar{g}_I\psi(v)}{c\tau_I}$
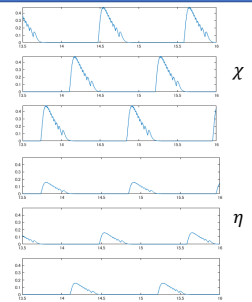
Can compute M from χ and η

Simulation

$$M = \begin{bmatrix} 0 & 3 & 0 \\ 0 & 0 & 3 \\ 3 & 0 & 0 \end{bmatrix}$$

1. Get v by simulating the network
2. Compute χ and η
3. Compute M from $M = \chi\eta^\dagger$

$$M = \begin{bmatrix} 4.61e-09 & 3.00 & -6.16e-12 \\ -6.11e-12 & 4.61e-09 & 3.00 \\ 3.00 & -6.06e-12 & 4.56e-09 \end{bmatrix}$$

χ

η

Summary

Objective
- identifying the network connection of spiking neurons in CPG

Progress
- harmonic balance has limitation when there are more than one input
- formulated equation that can compute M without using g_I and $\dot{v}$

Future work
- try if we can use sinusoidal approximation of v for 2ⁿᵈ approach

Observing the Selectivity of an Electron's Spin by an Organic Chiral Molecule

Hiroshi Goto
University of California, Los Angeles
Department of Electrical And Computer Engineering
Device Research Laboratory
Supervisor: Prof. Kang L. Wang

Device Research Laboratory

p. 1

Undisclosed

<3> Findings through JUACEP

3-1. Students' Reviews

Findings through JUACEP in UCLA

Name: Yusuke Terai
Affiliation at Nagoya University: Department of Micro-Nano Mechanical
Science and Engineering
Participated program: Medium course 2021-2022
Research theme: Bio-sample droplet evaporation with LASER
irradiation to induce salt precipitation aside and
improve SERS throughput
Advisor at the visiting university: Prof. Ya-Hong Xie
Affiliation at visiting university (Dept & Univ): Department of Materials
Science and Engineering, University of California, Los Angeles

I have lots of precious experience through JUACEP. I would like to write about what I found and feel in the laboratory and outside of the laboratory.

Regarding the laboratory, I have two topics to write. First thing is about the career. Our research group have 5 PhD students and they are 26-30 years old students. Some of them already got married and have children. They are so motivated to research and publish the papers so that they graduate earlier and finally get a job in the U.S. They sometimes wondered why most of Japanese graduate students in engineering don't try doctor course and look for jobs in Japan without thinking about being global works. I realized the big difference of career from Japan and the U.S. The second thing is how hard I research. Our lab do Raman measurements for biological samples while I belong to tribology (whose domain is functional surface, friction, surface coating or something like that) lab in Nagoya university. Therefore, I firstly struggled to plan my own research and catch up the discussion held every week. Through hard working and communication with group members, I managed to finish my research with group members help. I believe that this process made me grow up and confident myself. Researching was not easy at all, but I liked that time and it had motivated me to be a global worker in the future.
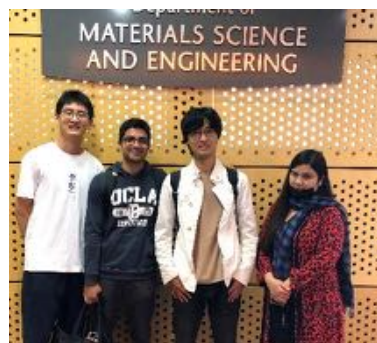
Regarding the life in LA, I would like to introduce people in LA and the exciting places. People are so friendly to me. We can enjoy talking with them and notice the difference of cultures in the conversations. Besides, people in LA are also so kind. They are not limited only roommates, but also everyone such as clerk, even someone I met first time. They sometimes voluntarily helped me when I looked in trouble like losing way or bike malfunction. I really like their communication culture. On the other hand, LA has also a bad aspect. LA is known as less safe city. I had my bike stolen and faced some scary situation in public transportation. My friend who is native in LA often tell me that we shouldn't use transportation.

Talking about having an exciting time, I made many good friends there. The applicant to JUACEP this year was only me. That's why, it was opportunity to make friends there and improve my English as a result. Additionally, LA has many entertaining places and great national parks. I especially highly recommend going to the baseball stadium, beautiful parks with friends!

I really appreciate everyone supported me to research in UCLA. Thanks to this program, I have a whole bunch of wonderful memories. I think I got flexibility, toughness, and additional perspective. Therefore, I'm sure that my experiences in LA will help me to study in Nagoya university and work in the company in the future.

Poutine life in Montreal

Name: Hirofumi Amada
Affiliation at Nagoya University: Chemical Systems Engineering
Participated program: Short course 2022
Research theme: Self-healing property of PEDOT:PSS film under high humidity
Advisor at the visiting university: Prof. Fabio Cicoira
Affiliation at visiting university: Chemical Engineering, Polytechnique Montreal

I can say that nothing could be comparable with what I experienced in Polytechnique Montreal. I studied self-healing property of PEDOT:PSS, which is one of the most common electro conductive polymers. Likewise, each student studies the material from his/her own perspective. One of intern students is a professional violinist and she was working on the development of sensors to detect the pressure of fingers while she is playing the violin. That is why I listened to solo-violin concert while I was working on my project sometimes, which is one of the most unique experiences I can never have in Japan. I really enjoyed my research and learned how I can cooperate with people from other countries.

Also, I really enjoyed the cultural experience in Montreal with my friends. Historically, Quebec province was colonized by France. That is why people in Montreal have French roots and there are lots of French culture all over the city. For example, what makes me really impressed is that I saw lots of artworks everywhere in the city. There are some paintings on the wall of high building (normally building is also European style) or sometimes on a street like shown in the pictures below. Also, there are beautiful parks everywhere in Montreal where many people have dinner, do BBQ or whatever they want. Normally I go to one of the parks with my friends with some cheese, cookies and some drinks in the weekend. I also got a tasty ice cream at the small shop in the park sometimes. Actually, I studied abroad in America as an exchange student when I was in undergraduate. Considering the experiences, I can say Montreal is really different from America and it is much more like European countries. In summary, I recommend you study abroad in Montreal and guarantee you will have a great experience there.

Finally, I would like to show gratitude for those who supported me and this program. In lab, Professor Fabio organized our project and gave us a lot of tips for the experiment. Ph.D. student Jinsil supported me in the way that she taught me how to use the equipment and discussed my project. Also, all of the lab members supported me so that I could enjoy my lab work in Montreal. Also, I really appreciated for advisors in both country (Canada and Japan). Advisor Annick in Montreal provided me with information necessary and Advisor Kim-Lee in Montreal helped me with the life in Montreal officially and privately. Advisor Kato-san and Leleito-sensei in Nagoya helped me with essential procedure for this project and Grib-sensei checked my essay, which is one of the most important submissions. I would not be able have such a great experience without their kind supports.
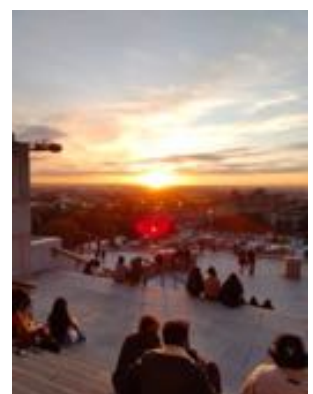
Findings through JUACEP

Name: Kentaro Takagi
Affiliation at Nagoya University: Dept. Mechanical Systems Engineering
Participated program: Medium-term course 2022

Research theme: Identifying relation between CPG network and oscillation profile
Advisor at the visiting university: Prof. Tetsuya Iwasaki
Affiliation at visiting university: Dept. Mechanical Aerospace Engineering, UCLA

My life in LA was challenging and memorable. When I was an undergrad, I was joining tennis club, so I played tennis almost every day and studied like other students did. It was satisfying life, but after I retired from the tennis club, I started to worry about my future. I thought changing environment that is currently surrounding me would help me interact with many people with different backgrounds and would open my world in a good way. In addition, I thought doing research in English is one of the most effective ways to improve my English. From these thoughts, I decided to join this program. As a result, I was able to learn many things and I could say for sure that I spent the best half year in my whole life.

The research life in UCLA was challenging and exciting. The part I struggled the most was discussing with Professor. I needed to study technical terms in English and had to practice explaining what I did briefly in English. Although it was difficult, this effort improved my communication skill a lot. The exciting part is talking with my lab mates. Since there are only 2 members other than me and they are PhD students, I was able to talk with them a lot and get inspiration from them. They told me how good it is to be a PhD student. I started to think going to PhD is a good option.

I had amazing roommates, so I was able to enjoy my life in LA. Two of my roommates were both from India, so I learned many Indian culture from them, especially food. We went various places in LA and ate and drunk together on weekends. I talked with them every day with English which helped me improve English.

Findings through JUACEP

Name: Hiroshi Goto
Affiliation at Nagoya University: Dept. Applied Physics
Participated program: Medium course 2022
Research theme: Observation of the chiral-induced spin selectivity effect
regarding an organic chiral molecule
Advisor at thevisiting university: Prof. Kang L. Wang
Affiliation at visiting university (Dept & Univ):
UCLA, Department of Electrical & Computer Engineering

My life as an international student of UCLA was wonderful. Honestly speaking, I had bigger worries than expectancies at first as I had never visited the U.S., much less lived there until then. Furthermore, my English was not good. However, such worries were gone soon thanks to my roommates, colleagues, and friends with whom I met some communities although it took some time to adapt. I would like to share my experience below briefly through this program. Anyway, I could have spent good time in LA and certain that my decision was right. I would like to thank all of them and JUACEP Officer.

1. Research in UCLA

My exchange program offer was accepted by Prof. Kang L. Wang, and I belonged to Device Research Laboratory (DRL). It consists of three groups, spintronics group which I joined, topological group and AI group. First month, I struggled to communicate with colleagues and learn how to use experimental equipment. Honestly speaking, it was also hard to attend weekly group meeting and entire meeting every Tuesday and Friday, however, I could have gotten not only knowledge or advise regards with my research but also motivated to do my research thanks to their enthusiasm for their research. I would like to thank Prof. Kang L. Wang for giving me such an amazing opportunity. Also, I'm thankful for kindness of DRL members.

2. Daily life in the U.S.

I could get along with my roommates soon and we often went out together in weekends. In holidays, we had special dish and explored around Los Angeles such as Santa Monica, Culver City, Beverly Hills and downtown. Also, I joined Japan Student Association and soccer community, and made friends there. They are great guys, and it was interesting to know about their histories.

Talking about the hard point of my life in LA, price of everything was so high due to worst depreciation of the yen ever recorded and price increases. In the U.S, the price of eating out is originally high compared with Japan and even in the fast food, it costs at least $10 that is converted more than 1,500 yen at that time. Thus, I cooked almost every dish by myself in order to save money. Although that was hard for me, that became a good experience including finding out the difference between an American supermarket and a Japanese one and being taught how to make an Indian dish by Indian roommates. I recommend going to a grocery store and try many kinds of food you have not eaten ever in Japan. You can visit a large grocery store called "Ralphs" near the UCLA and a Japanese supermarket called "NIJIYA" in Sawtelle if you want to get Japanese stuff.
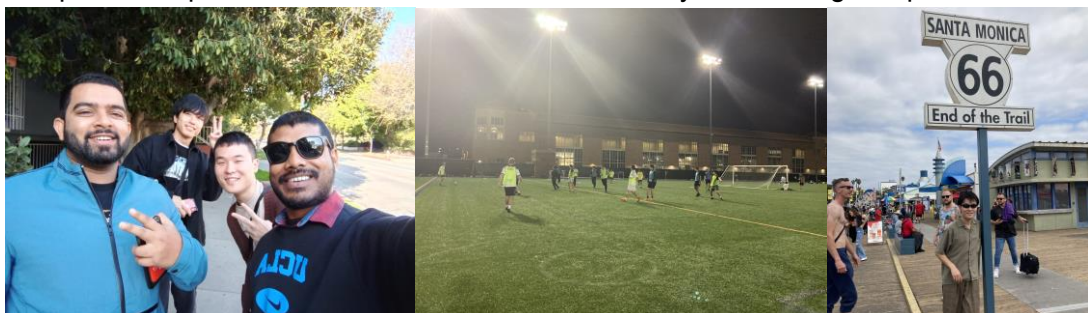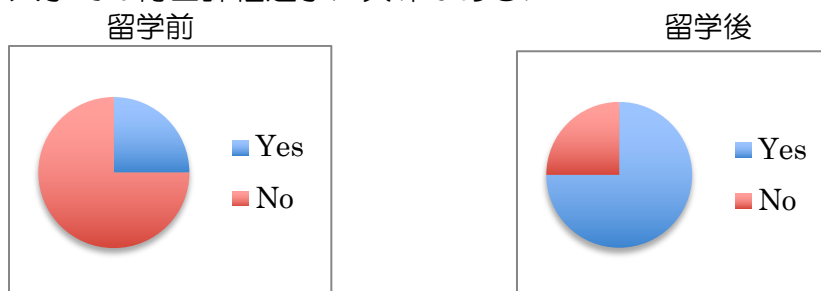
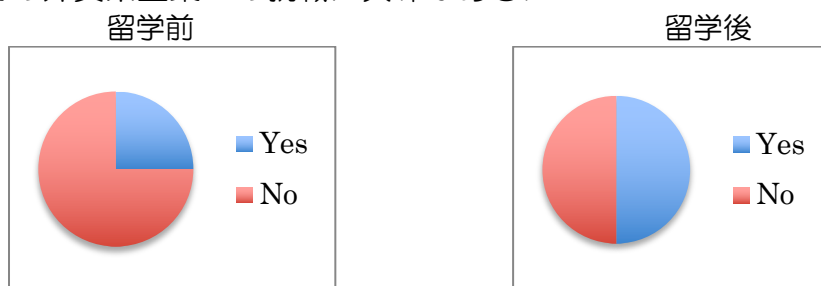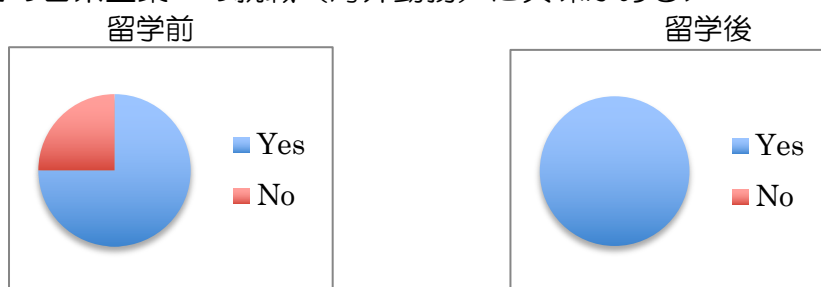## 3-2. Questionnaires

派遣プログラム参加者に行ったアンケート結果

＜博士課程進学に興味がある＞

留学前 / 留学後
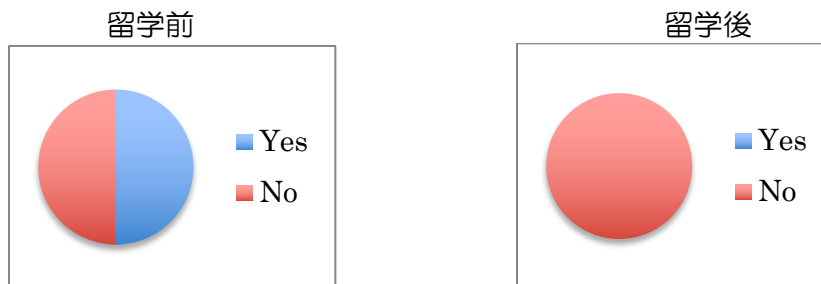
＜外国の大学での博士課程進学に興味がある＞

留学前 / 留学後

＜日本での外資系企業への就職に興味がある＞

留学前 / 留学後

＜外国での日系企業への就職（海外勤務）に興味がある＞

留学前 / 留学後

＜外国での日系以外の企業への就職に興味がある＞

留学前 / 留学後
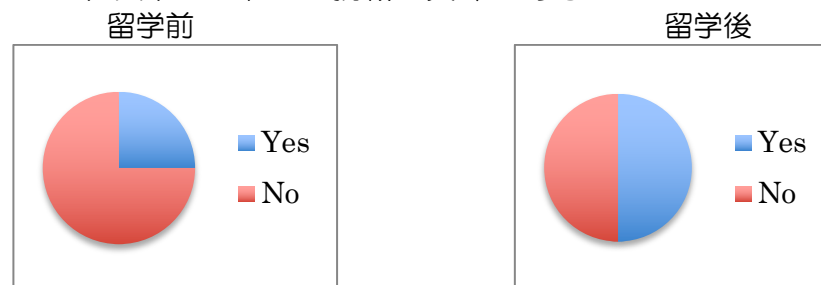
<u>アンケート結果まとめ</u>　博士後期課程を目指す学生は国内で長年減少傾向だが，現地の研究チーム内で博士課程学生の役割・取組を目にして刺激を受け，外国での博士課程に興味を抱くようになる学生が毎年いる．また帰国後に外資系企業への就職や海外勤務に関心を持つようになることがアンケートで読み取れる．

3-2. Questionnaires

1. このプログラムの良かった点

- 受入先大学で正規学生と同等の立場で研究活動をすることができる。

- 研究しながら留学できる。

- 単位が取れる

- 就活のタイミングと被らない。

- 研究プログラム特有のタスクや制限がなく、基本的に研究活動に従事するので集中できる。旅行なども自由にできる。

- 現地大学在籍のコーディネータ教員がいる、随時JUACEP事務室とメールやLineでやりとりできる、などサポート体制が整っていて安心して留学生活を送れる。

- JASSOからの追加支援も手配してもらって助かった。

2. このプログラムで改善してほしい点

- 寮が用意されていると、他大学の留学生との交流が深まると思う。

- Polytechnique Montrealと協定校になると、もっと留学しやすくなると思う。（2023年から協定校になりました）

- 研究活動の全ての時間を自分の研究に充てることができず、他の学生のサポートをする必要があった。JUACEPの期間は限られているので、自分の研究に集中したかった。（と言っても教授や研究室の状況によるので解決しきれない問題だとは思う）

- 宿舎を見つけるサポートを充実させてほしい。自分の場合は、先に出発していたJUACEPメンバーの所に一緒に住めたので結果的には大きな苦労はなかったが、1年契約のためサブリースする相手を探さなければならなかった。時期にもよるが、部屋が見つからない可能性もあると思う。土地勘のない場所で希望の物件を探すのは非常に困難なので、候補物件や大学周辺の様子をビデオなどで事前に見られたらよかった。

3. 住居について［A］宿舎の見つけ方・宿舎形態・家賃・大学までの足　［B]感想

- ［A］ネットで探した。370CAD/月。大学まで徒歩 20 分。
［B］インターネットで決める場合は、口頭でなく必ず契約書類を作ることをお勧めします。そうでないと私のように、大家が家賃をより多く払う人を勝手に見つけてきて追い出される危険性があります。モントリオールの場合は、可能なら寮に入ることを強くお勧めします。

- ［A］ネットで「Los Angeles shared room」で検索し、びびなび、Claigslist, Spareroom を利用した。最終的には Sota colving という会社を利用してルームシェアに決めた。824USD/月。大学まで自転車 40 分。

3-2. Questionnaires

　　［B］まず候補になる家を探すところから大変である。メールの返信
がないこともあり苦労した。

・　［A］UCLA 近辺を歩いて探した。シェアハウス。660USD/月。大
学まで徒歩 10 分。
　　［B］最初はホテルに泊まりながら探した。たまたまルームメイトを
見つけることができ、UCLA 近辺のアパートの一室を借りて過ごす
ことができたので良かったが、運がなかったらかなり大変だったと
思う。Claigslist などがあるが信頼性は低いので、UCLA housing
という Facebook のグループに入ってルームメイトを探すのが一番
いいと思う。

・　［A］知人の部屋に同居。シェアハウス。660USD/月。大学まで徒
歩 15 分。
　　［B］大学にも食料品店にも非常に近く、治安もかなり良い場所でした。基本的に住人は UCLA
の学生と思われる人で、特に近隣トラブル等もありませんでした。また、ディスポーザが壊れ
たりやトイレの配水管が壊れるなど一部欠陥があ離ましたが、大家さんが丁寧に対応してくれ
て問題とはなりませんでした。

4．滞在中の印象深いことなど

・　ルームメイトがフレンドリーで毎日が楽しかった。色々な人と出会えて刺激になった。

・　大学について言えば、まずはキャンパスの広さと綺麗さに驚きました。私は大学のグラウンド
でよくサッカーをしていたのですが、整備された人工芝のグラウンドでとても快適でした。現
地の友人に聞いた話によれば、プロサッカーチームもシーズンオフ中に練習をしに来ることが
あるそうです。また、私が所属した研究室に関しては、メンバーの研究に対する熱意に圧倒さ
れました。毎週ミーティングがあるのですが、2 時間のミーティングが終わった後も議論し続
ける姿には驚くと同時に、自分の研究に対するモチベーションの向上にも繋がりました。ロサ
ンゼルスの悪い印象としては、やはりホームレスの多さです。大麻の匂いや大きな叫び声が聞
こえるなど少々危険を感じました。ただ、夜に一人で帰宅する事もあるくらい、大学近辺は
かなり治安が良いです。

・　教授は常に論文投稿を目指す前提でミーティングを行っていました。私の研究成果についても
教授が論文化を目指しているため、留学終了後もオンラインミーティングをすることになりま
した。

・　Hello talk や Tinder など、オンライン上で知り合った人たちと友達になってたくさん楽しい
思い出をつくることができた。

・　買った自転車が翌日に盗まれた。家の前に停めていたらチェ
ーンが切られていた。チェーンは良いものを選ぶべき。そし
て極力室内に停めるべき。

・　ホームレスが多く、歩くのが怖い道路が多いこと。

・　夏のロサンゼルスの朝と夜は意外と寒いこと。

・　物価が高い+円安の影響で留学費用はかなり大きいこと。

・　研究室内の実験装置は限られているので、他の教授にアポイ
ントメントをとる必要があること。

3-2. Questionnaires

５．その他，自由コメント

- 当初は不安だらけでしたが、JUACEP 事務室の方をはじめ多くの人のサポートのお陰で大変貴重な経験をする事が出来ました。アメリカの文化に触れられただけでなく、人の温かさを感じられ、留学して本当に良かったと感じています。本当にありがとうございました。

- UCLA での研究でしか得られない貴重な経験ができました。今後の人生においてこの経験が及ぼす影響はかなり大きいと考えます。８か月という期間はアッと今に過ぎました。コロナ禍ということもあり、プログラムが開かれるか不安でしたが諦めないで良かったです。

- ありがとうございました。